UNIVERZITA KARLOVA V PRAZE
Přírodovědecká fakulta

Katedra anorganické chemie

Termodynamické studie makrocyklických ligandů odvozených od cyclamu

Rigorózní práce

Jana Havlíčková

Praha 2008

Prohlášení

Prohlašuji, že jsem tuto rigorózní práci vypracovala samostatně, a že jsem všechny použité prameny řádně citovala.

Jsem si vědoma toho, že případné využití výsledků, získaných v této práci, mimo Univerzitu Karlovu v Praze je možné pouze po písemném souhlasu této univerzity.

V Praze dne 15. července 2008

Jana Havlíčková

podpis 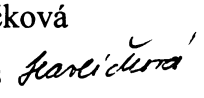

Obsah

1 Úvod

V současné době neustále roste zájem o makrocyklické polyaminy, což je dáno jejich biologickými vlastnostmi a významem v oblasti koordinační chemie. Jejich komplexy s různými ionty kovů nacházejí uplatnění především v medicíně jako kontrastní látky pro NMR tomografii, v radioterapii a radiodiagnostice, jako látky působící proti viru HIV, ale také při transportu iontů kovů a atomu kyslíku v biologických systémech atd.[1]

Všechny látky používané v klinické medicíně musí splňovat celou řadu požadavků. Musí být dostatečně stabilní *in vivo*, protože velká část používaných iontů kovů je toxických. Tyto komplexy nemusí být v daném systému termodynamicky nejstabilnější, postačuje pouze kinetická inertnost.[2] Podmínky *in vivo* nejsou sice nijak extrémní (pH přibližně 7, teplota kolem 37 °C), ale je nutno brát v úvahu možnost kysele katalyzované hydrolýzy díky poklesu pH v některých tkáních. Vzhledem k relativně vysoké koncentraci některých iontů v organismu (například Na^{+}, K^{+}, Mg^{2+}, Ca^{2+}, Zn^{2+}, $Fe^{2+/3+}$, Cu^{2+} atd.) je třeba brát v úvahu možnost případné konkurenční komplexace.[2] Podobně je v organismu přítomno mnoho různých konkurenčních ligandů (cukrů, organických kyselin, aminokyselin, bílkovin; například transferrin).

1.1 Radiofarmaka

Radiofarmaka jsou léky obsahující radionuklid, které se používají v nukleární medicíně k diagnóze a léčbě různých onemocnění. Jedná se především o malé organické či anorganické sloučeniny o definovaném složení. Mohou to být též makromolekuly (např. monoklonální protilátky), které nejsou stechiometricky značené radionuklidem. Na základě jejich medicínské aplikace je lze rozdělit do dvou hlavních skupin (látky diagnostické a terapeutické).

Pro diagnostické účely se používají molekuly značené izotopy, jež emitují γ záření (pro metodu SPECT – „Single-photon emission computed tomography“) nebo izotopy emitující β^{+} záření (pro metodu PET – „Possitron emission tomography“). Tyto látky se používají ve velmi nízkých koncentracích a nemají tedy farmakologický efekt. Cílem jejich použití je detailní popis orgánů a tkání a především testování jejich fyziologických funkcí během akumulace radioaktivního indikátoru. Radiodiagnostika představuje neinvazivní metodu hodnotící stav onemocnění a monitorující efekt léčby.

Terapeutickými radiofarmaky jsou molekuly navržené tak, aby doručily terapeutickou dávku ionizujícího záření do specifického místa onemocnění. Hlavními překážkami v radioterapii jsou dostupnost terapeutických izotopů a techniky pro jejich specifickou lokalizaci v postižené tkáni (např. nádoru).

1.2 Zobrazovací metody

1.2.1 Pozitronová emisní tomografie (PET)

Pozitronová emisní tomografie je neinvazivní vyšetřovací zobrazovací metoda. Na rozdíl od jiných zobrazovacích metod, které umožňují pouze identifikaci anatomických struktur, PET zhodnotí i metabolickou aktivitu buněk a s vysokou přesností upozorní na funkční změny orgánů.

PET používá radiofarmaka značená radionuklidy, které se rozpadají za vzniku pozitronu. Při positronové anihilaci vznikají dva kolineární fotony (fotony, jejichž dráhy leží na stejné přímce, ale směr jejich pohybu je opačný) o energii 511 keV, což umožňuje přesnější určení místa jejich vzniku.[3]

V současné době se dává přednost radionuklidy značeným malým peptidům před značenými proteiny či protilátkami. Nejlepším kandidátem pro značení peptidů se zdá být ^{18}F díky jeho vhodným fyzikálním a jaderným vlastnostem. Hlavní nevýhodou peptidů značených ^{18}F je jejich pracná a časově náročná příprava. Problémem je rovněž *in vivo* stabilita a vliv na biologické chování molekul.[4] Spolu s ^{18}F je v současné době nejpoužívanějším β^+ emitorem ^{11}C. Dalšími vhodnými izotopy by mohly být ^{55}Co, ^{68}Ga a ^{110m}In. Hlavní nevýhodou izotopů ^{55}Co a ^{110m}In je jejich obtížná dostupnost. Některé z těchto radionuklidů také emitují γ záření, které může ovlivnit měřící vlastnosti PET.[5]

1.2.2 Jednofotonová emisní počítačová tomografie (SPECT)

Tato metoda je založena na detekci γ záření vhodných izotopů, které jsou vpraveny do těla pacienta. Počítačové zpracování umožňuje vytvářet dvou- nebo třírozměrné obrazy procesů, např. v mozku. Není určena pro zobrazování anatomie. Nejpoužívanějším radionuklidem pro diagnostické účely je ^{99m}Tc díky jeho optimálním jaderným vlastnostem, snadné dostupnosti a nízké ceně. Dalším radionuklidem vhodným pro γ zobrazovací techniky je ^{111}In.

1.3 Radioimunoterapie

Při radioimunoterapii je třeba dopravit do cílové oblasti maximální radiační energii a omezit působení záření pouze na požadovanou oblast. Vhodné izotopy jsou tedy β^- nebo α emitory bez (nebo s nízkým) doprovodným γ zářením.[6] U γ zářičů lze využít emise Augerova elektronu. Dosah těchto částic se ve tkáních pohybuje řádově v setinách milimetru u α zářičů a v desetinách až jednotkách milimetru v případě β^- zářičů.[2]

1.3.1 Radionuklidy emitující α záření[7]

Přestože α částice vykazují vysokou *in vitro* a *in vivo* cytotoxicitu, je jejich použití, vzhledem k nebezpečným dceřiným produktům u většiny z nich, velmi problematické. Snad pouze ^{211}At a ^{212}Bi se z tohoto hlediska zdají být možnými kandidáty. Sloučeniny astatu však nejsou za podmínek *in vivo* příliš stabilní.[6] Izotop ^{212}Bi má sám o sobě příliš krátký poločas rozpadu (cca 1 h) a musí se aplikovat ve formě svého prekurzoru, tedy ^{212}Pb.[8] Pro radioimunoterapii byly též navrženy α emitory s delším poločasem rozpadu $^{252/255}$Fm, ^{246}Cf a ^{225}Ac.

1.3.2 Radionuklidy emitující β^- záření[7]

β^- částice mají relativně velkou penetraci do tkání, a to je předurčuje pro použití i u velkých nádorů s velkou heterogenitou. I když jsou β^- zářiče heterogenně rozptýleny v cílové tkáni, poskytují díky této vlastnosti víceméně homogenní dávku záření.[9] Výběr konkrétního radioizotopu záleží na velikosti a umístění nádoru. Nízkoenergetické β^- emitory (např. ^{131}I) jsou nejvhodnější pro malé nádory ($d \approx 1$–2 mm). Středněenergetickými β^- emitory používanými v klinické medicíně pro kostní metastázy jsou ^{153}Sm a ^{186}Re. Do skupiny vysokoenergetických β^- emitorů patří např. ^{32}P, ^{89}Sr a ^{90}Y. Tyto jsou používány pro léčbu velkých nádorů ($d \geq 1$ cm).

1.3.3 Zářiče Augerových elektronů[7]

Zářiče Augerových elektronů se zdají být velmi účinné, ale pouze tehdy, pokud se daný nuklid dostane přes buněčnou membránu až do bezprostřední blízkosti jádra. Vhodnými emitory Augerových elektronů se zdají být např. $^{193m/195m}$Pt a ^{125}I.

1.4 Radionuklidy

1.4.1 Dostupnost radionuklidů

Určujícími faktory použití radionuklidů jsou často cena a dosažitelná radiochemická a chemická čistota. Ideálním způsobem přípravy jsou radionuklidové generátory (např. $^{99}Mo/^{99m}Tc$ generátor a $^{68}Ge/^{68}Ga$ generátor), které jsou založeny na dlouho žijícím „rodičovském" izotopu. „Rodičovský" izotop se rozpadá na krátce žijící dceřiný radionuklid, který musí být lehce oddělitelný od svého prekurzoru buď pomocí iontoměniče (nejběžnější metoda), nebo extrakcí rozpouštědlem. Několik málo radionuklidů používaných v zobrazovacích metodách (gama scintigrafie a PET) je produkováno jadernými reaktory. Dalším způsobem produkce jsou urychlovače a cyklotrony. Tyto způsoby přípravy jsou však velmi drahé.

1.4.2 Stručný přehled nejpoužívanějších radioizotopů a jejich využití

Měď[10]

Měď poskytuje celou řadu radioizotopů s poločasem rozpadu od 9.8 min do 61.9 h, které mohou být použity jak k radiodiagnostickým, tak k radioterapeutickým účelům. Použití radionuklidů mědi má mnoho výhod oproti jiným radionuklidům. V chemii mědi dominují dva oxidační stavy (I a II) oproti oxidačním stavům např. Tc a Re (I–VII). Měď je třetím nejzastoupenějším kovem v lidském těle (po Fe a Zn) a je velmi dobře prostudována po stránce biochemie a metabolismu v lidském těle. Velmi dobře jsou známy i její koordinační a redoxní vlastnosti.

Izotopy ^{60}Cu a ^{61}Cu patří mezi β^+ emitory. Výzkum těchto izotopů je ve velmi ranném stadiu, a tedy nejsou známa jejich biologická a klinická použití. Díky snadné dostupnosti je izotop ^{62}Cu velmi nadějný pro použití v PET. Jeho krátký poločas rozpadu (9.74 min) je vhodný pro opakované studie za různých fyziologických podmínek. Nejvšestrannějším izotopem mědi je izotop ^{64}Cu díky jeho rozpadovému schématu, který zahrnuje elektronový záchyt, β^- a β^+ rozpad a také emisi Augerových elektronů. Je vhodný jak pro metodu PET, tak pro radioterapii. Izotop ^{66}Cu (β^- emitor) je vhodný pro radioterapii velkých nádorů (≥ 1 cm). Tento izotop je také možné použít společně s izotopem ^{64}Cu nebo ^{67}Cu pro zvýšení terapeutického účinku. Fyzikální

vlastnosti izotopu ^{67}Cu (β^- emitor) jsou velmi vhodné pro použití v oblasti radioimunoterapie.

Technecium

Technecium je jediný přechodný kov, který nemá žádný stabilní izotop. Radiofarmaka založená na ^{99m}Tc (γ emitor) jsou značně využívána pro zobrazování kostí, mozku, srdce, funkce ledvin a rakoviny prsu.[11]

Gallium[12]

Gallium poskytuje tři izotopy, které mají vhodné rozpadové charakteristiky pro využití v zobrazovacích metodách, jako je gama scintigrafie a PET. Izotop ^{66}Ga není zatím příliš využíván. Izotop ^{67}Ga byl v roce 1953 jako první použit pro humánní účely. ^{67}Ga značený citrát se využívá k diagnóze některých typů nádorových onemocnění jako je např. nádor plic, maligní melanom a leukémie. Izotop ^{68}Ga ($t_{1/2} = 68$ min) je produkován $^{68}Ge/^{68}Ga$ generátorem a rozpadá se z 89 % β^+ emisí. Díky jeho snadné dostupnosti a vhodnému poločasu rozpadu leží hlavní zájem ve vývoji ^{68}Ga značených myokardiálních a mozkových radiofarmak.

Indium[12]

Nejpoužívanějším izotopem india je ^{111}In. Tento izotop se rozpadá elektronovým záchytem následovaným emisí γ fotonů. Mnoho látek na bázi ^{111}In se v zobrazovacích metodách používá dodnes.

Yttrium[12]

Yttrium poskytuje dva izotopy použitelné pro přípravu radiofarmak. ^{90}Y (β^- emitor) je vhodný pro radioterapii, izotop ^{86}Y (β^+ emitor) se uplatňuje v PET.

1.5 Makrocyklické polyaminy

Chemie makrocyklů obsahujících ve své molekule atom dusíku je velice bohatá, především z důvodu, že není omezena pouze na jednoduché cykly. Díky trojvaznosti aminového atomu dusíku může docházet buď ke tvorbě složitých cyklů (rozvětvené, polycyklické), nebo, u nevětvených makrocyklů, k navázání tzv. pendantních skupin,

které mohou být schopny koordinace. Díky této vlastnosti mohou výrazně ovlivňovat selektivitu daného makrocyklického ligandu vůči různým kationtům, rychlost komplexací a stabilitu vznikajících komplexů. Mezi nejběžnější pendantní skupiny dusíkatých makrocyklů patří především karboxylové kyseliny (zbytek kyseliny octové, propionové; jejich deriváty, jako jsou amidy a estery), alkyly obsahující aminové funkce, dále alkoholy, fenoly, thioly a oxokyseliny fosforu, případně jejich estery. Makrocyklické polyaminy vykazují ohromnou schopnost vázat celou řadu iontů kovů, přičemž ve většině případů dochází při této vazbě ke konformačním změnám.[13] Oproti obdobným necyklickým ligandům vytváří makrocykly stabilnější komplexy díky tzv. makrocyklickému efektu. Makrocyklické ligandy jsou nejčastěji deriváty velmi dobře známých cyklických aminů: 1,4,7-triazacyklononan, 1,4,7,10-tetraazacyklododekan (cyclen) a 1,4,8,11-tetraazacyklotetradekan (cyclam) (Obr. 1).

1.5.1 Deriváty 1,4,7-triazacyklononanu

Deriváty 1,4,7-triazacyklononanu jsou ideální pro komplexaci trojmocného gallia a india. Komplexy Ga(III) a In(III) s 1,4,7-triazacyklononan-1,4,7-trioctovou kyselinou (H_3nota, Obr. 1) se používají v diagnostice některých nádorů.[2]

1.5.2 Deriváty cyclenu

Ligandy odvozené od cyclenu jsou schopny komplexovat všechny ionty kovů, ale nejvhodnější jsou pro trojmocné ionty lanthanoidů, které vyžadují vyšší koordinační čísla. Příkladem takového ligandu může být 1,4,7,10-tetraazacyklododekan-1,4,7,10-tetraoctová kyselina[14] (H_4dota, Obr. 1). Komplex paramagnetického iontu Gd(III) s H_4dota a s jejím analogem H_3do3a (1,4,7,10-tetraazacyklododekan-1,4,7-trioctová kyselina, Obr. 1) se používají pro přípravu kontrastních látek v NMR tomografii.[12, 15] Vyšší selektivitu a vhodnou termodynamickou stabilitu vykazují komplexy ligandů s pedantními skupinami obsahujícími fosfor. Velmi dobře prostudovanými ligandy vhodnými pro ionty lanthanoidů jsou 1,4,7,10-tetraazacyklododekan-1,4,7,10-tetrakis(methylfosfonová kyselina) (H_8dotp, Obr. 1) a její deriváty.[16]

1.5.3 Deriváty cyclamu

Cyclam a ligandy od něj odvozené vytváří velmi ochotně komplexy s ionty přechodných kovů, často s velmi vysokou termodynamickou a kinetickou stabilitou. Ligandy s cyclamovým skeletem disponují makrocyklickou kavitou, jejíž velikost je optimální pro ion Cu(II). Cyclam vytváří s mědí vůbec nejstabilnější známé komplexy ($\log K = 28.1$)[17], avšak kinetika komplexace je relativně pomalá. Proto se používají deriváty s různými pendantními skupinami, nejčastěji s acetáty, které urychlují kinetiku komplexace. Příkladem může být 1,4,8,11-tetraazacyklotetradekan-1,4,8,11-tetraoctová kyselina[14] (H_4teta, Obr. 1). Dalším ligandem vhodným pro $^{64/67}$Cu je např. 4-[(1,4,8,11-tetraazacyklotetradec-1-yl)methyl]benzoová kyselina[2] (Hcpta, Obr. 1). Z fosforových derivátů jsou pak dobře prostudovány např. H_8tetp[18] (1,4,8,11-tetraazacyklotetradekan-1,4,8,11-tetrakis(methylfosfonová kyselina), Obr. 1) a 1,8-H_4te2p[19] (1,4,8,11-tetraazacyklotetradekan-1,8-bis(methylfosfonová kyselina), Obr. 1). Deriváty cyclamu (především s methylenfosfonovými pendantními skupinami) se používají také pro komplexaci technecia.[20]

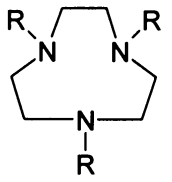

R = H 1,4,7-triazacyklononan
R = CH_2COOH H_3nota

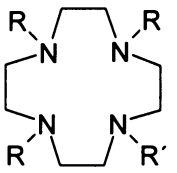

R = R′= H cyclen
R = R′= CH_2COOH H_4dota
R = CH_2COOH, R′= H H_3do3a
R = R′ = $CH_2PO_3H_2$ H_8dotp

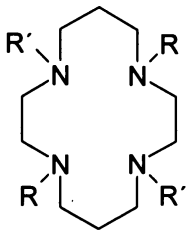

R = R′= H cyclam
R = R′= CH_2COOH H_4teta
R = R′= $CH_2PO_3H_2$ H_8tetp
R = $CH_2PO_3H_2$, R′= H 1,8-H_4te2p

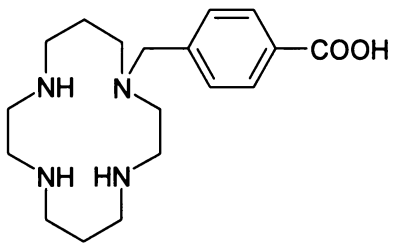

Hcpta

Obr. 1: Strukturní vzorce výše zmíněných ligandů

2 Výsledky a diskuze

V této kapitole budou porovnány acidobazické a komplexotvorné vlastnosti studovaných ligandů s vybranými strukturně příbuznými ligandy. Pro ostatní ligandy byla vybrána taková data, která byla získána za podmínek co nejbližších k titracím studovaných ligandů, tj. při teplotě 25 °C a iontové síle 0.1 mol dm^{-3} (KNO_3).

2.1 Acidobazické vlastnosti makrocyklických polyaminů

Protonizační konstanty studovaných ligandů (Obr. 2) jsou uvedeny v Tab. 1. Disociační konstanty studovaných ligandů a vybraných strukturně podobných ligandů (Obr. 1 a Obr. 2.) jsou uvedeny v Tab. 2.

Tabulka 1: Protonizační konstanty studovaných ligandů

(T = 25.0±0.1 °C, I = 0.1 mol dm^{-3} KNO_3)

Konstanty	1,4-H_4te2p	1,8-H_4^{Me2}te2p	1,8-H_2^{Et2}te2p
logβ_1	—	11.47 (1)	11.62 (1)
logβ_2	25.72 (3)	23.642 (3)	21.92 (2)
logβ_3	32.282 (8)	30.840 (6)	22.5 (1)
logβ_4	37.470 (9)	37.166 (5)	—
logβ_5	39.77 (1)	38.69 (1)	—
logβ_6	—	39.54 (8)	—

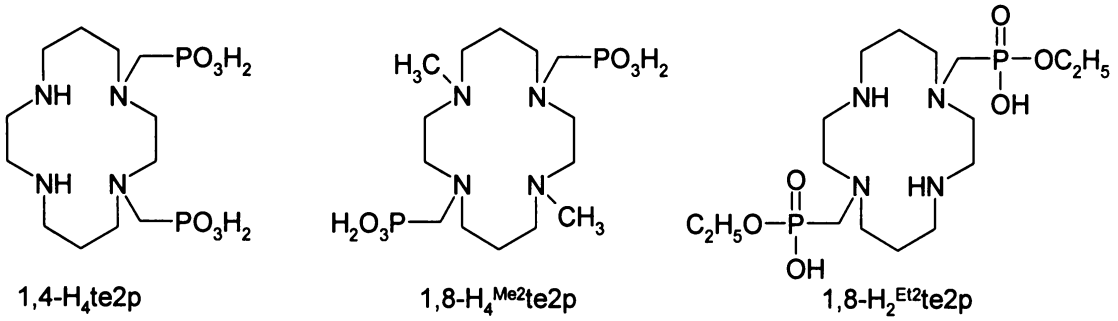

Obr. 2: Strukturní vzorce studovaných ligandů

Tabulka 2: Disociační konstanty studovaných a strukturně blízkých ligandů (T = 25.0±0.1 °C, I = 0.1 mol dm^{-3})

pK_a	1,4-H_4te2p	1,8-H_4^{Me2}te2p	1,8-H_2^{Et2}te2p	1,8-H_4te2p[19]	cyclam[21]	H_4teta[22]	H_8tetp[23]
pK_1	—	11.47	11.62	—	11.29	10.68	13.4
pK_2	25.72	12.17	10.30	26.41	10.19	10.14	12.8
pK_3	6.56	7.20	0.6	6.78	1.61	4.09	8.82
pK_4	5.19	6.33	—	5.36	1.91	3.35	7.75
pK_5	2.30	1.52	—	1.15	—	—	6.25
pK_6	—	0.85	—	—	—	—	5.42

Schéma postupné deprotonizace tetraazamakrocyklických sloučenin bylo popsáno a prokázáno NMR například pro ligandy H_4dota, H_4teta, H_8dotp a H_8tetp.[14c, 19] U studovaných ligandů probíhá deprotonizace obdobným způsobem (viz Příloha).

První dvě protonizační konstanty u 1,4-H_4te2p a 1,8-H_4te2p (pK_a = 25.72, respektive 26.41) odpovídají protonizacím dvou sekundárních aminových skupin cyklu. Protože k protonizaci dochází téměř současně, je možno určit pouze jejich sumu (pK_1 + pK_2). Skutečnost, že se jedná o protonizaci sekundárních, nikoliv terciárních dusíků cyklu, byla ověřena u 1,8-H_4te2p[19] na základě změn chemických posunů fosforu a protonů pendantního methylenu v závislosti na –log[H^+] v rozmezí 11.5 až 13. První dvě protonizační konstanty azacyklů mívají obvykle vysokou hodnotu (pK_a > 12).[18b] K jejich stanovení se pak používá „kvantitativní" NMR titrace (viz Příloha).

U 1,8-H_4^{Me2}te2p má první konstanta (pK_1 = 11.47) výrazně nižší hodnotu než konstanta odpovídající následné protonizaci (pK_2 = 12.17). Toto převrácení „klasické" posloupnosti hodnot protonizačních konstant bylo již pozorováno u některých makrocyklických sloučenin a je zdůvodňováno změnami konformace makrocyklu při jednotlivých protonizacích.[23, 24] Takové převrácení bylo zjištěno i u ligandu 1,8-H_4te2p a je vysvětleno snížením rigidity skeletu ligandu po první deprotonizaci z atomů dusíku, což má za následek labilizaci vodíkové vazby (mezi atomy dusíku sekundárních aminových skupin a atomy kyslíku pendantních fosfonátových skupin; viz Příloha) a tedy i snadnější odštěpení posledního protonu.[19] Převrácené hodnoty konstant jsou též popsány i u samotného cyclamu.[24b] Tento efekt se zdá být charakteristický pro deriváty

cyclamu pravděpodobně díky uspořádání ethylenových a methylenových řetězců mezi atomy dusíků v kruhu.[19]

Při vzájemném porovnání prvních dvou protonizačních konstant (pK_1 a pK_2) ligandů s pendantními fosfonátovými skupinami je patrné, že nejnižší konstanty náleží ligandům 1,8-H_4^{Me2}te2p a 1,8-H_2^{Et2}te2p. V obou případech je důvodem větší odčerpání elektronové hustoty z atomů dusíku kruhu zavedením methylové skupiny, popřípadě fosfonové monoesterové skupiny. Zavedením methylové skupiny u 1,8-H_4^{Me2}te2p vznikají terciární aminové skupiny, kterým odpovídají nižší hodnoty pK_a. Methylové skupiny jsou navíc stericky náročnější než atomy vodíku. V případě 1,8-H_2^{Et2}te2p se tvoří slabší vodíkové vazby, což má za následek opět snížení hodnot pK_a pro atomy dusíku sekundárních aminových skupin. Velmi nízká protonizační konstanta pK_3 u 1,8-H_2^{Et2}te2p ($pK_3 = 0.6$) náleží buď protonizaci fosfonátové skupiny, nebo protonizaci terciární aminové skupiny, která má sníženou bazicitu díky přítomnosti fosfonové monoesterové skupiny.

Všechny ligandy obsahující pendantní fosfonátové skupiny mají hodnoty pK_1 a pK_2 vyšší než samotný cyclam. Naopak je tomu u ligandu s pendantními acetátovými skupinami (H_4teta). Bazicita aminových skupin klesá v pořadí aminofosfonová > aminokarboxylová > aminofosfinová. Tento trend je velmi dobře znám[25], vyšší bazicita aminové skupiny aminofosfonových skupin je vysvětlena delokalizací záporného náboje skupiny $-PO_3^{2-}$. Na bazicitu aminové skupiny aminofosfinových kyselin má také vliv substituent na atomu fosforu. Bazicita stoupá v pořadí substituentů H < fenyl < methyl < *terc*-butyl.[26] Vyšší hodnota pK_1 a pK_2 u ligandů s pendantními fosfonátovými skupinami ve srovnání se samotným cyclamem je pravděpodobně dána též tvorbou výše zmíněných intramolekulárních vodíkových vazeb.

2.2 Komlexotvorné vlastnosti makrocyklických polyaminů

Z hlediska komplexačních vlastností mají v případě těchto ligandů velký význam komplexy s ionty přechodných kovů, neboť polyazacykly s pendantními skupinami schopnými koordinace jsou výbornými ligandy právě pro ionty přechodných kovů a také pro ionty lanthanoidů.

Konstanty stability komplexů ($\log\beta_{011}$) studovaných a strukturně příbuzných ligandů jsou uvedeny v Tab. 3.

Ve většině případů bylo možné stanovit konstanty stability komplexů studovaných ligandů přímou titrací. U systémů s pomalou kinetikou muselo být použito tzv. metody „out-of-cell" (viz Příloha). V případě 1,4-H_4te2p se jednalo pouze o systém s Ni(II). U ligandu 1,4-H_4^{Me2}te2p to byly systémy s Cd(II), Cu(II), Zn(II), Co(II) a Ni(II). Pomalou kinetiku komplexace vykazoval i systém 1,8-H_2^{Et2}te2p s Zn(II). U systémů ligandů 1,4-H_4^{Me2}te2p a 1,8-H_2^{Et2}te2p s Ca(II) muselo být použito nadbytku Ca(II), aby vznikl komplex v dostatečném zastoupení.

Tabulka 3: Hodnoty $\log\beta_{011}$ komplexů vybraných ligandů
(T = 25.0±0.1 °C, I = 0.1 mol dm^{-3})

Ligand	Cu(II)	Zn(II)	Ni(II)	Co(II)	Cd(II)	Pb(II)	Ca(II)
1,4-H_4te2p	27.21	20.16	21.92	—	17.03	12.85	3.45
1,4-H_4^{Me2}te2p	24.03	17.56	15.55	15.66	15.89	12.79	3.98
1,8-H_2^{Et2}te2p	19.68	15.59	—	—	—	10.59	1.92
1,8-H_4te2p	25.40[27]	20.35[27]	21.99[27]	19.28[27]	17.89	14.96	5.26
cyclam[17]	28.1	15.2	22.2	14.3	11.3	10.9	—
H_4teta[22, 28]	21.6	16.27	19.91	16.56	18.02	14.32	8.32
H_8tetp[29]	26.6	17.6	15.6	15.3	16.7	15.5	—

Komplexy ligandu 1,8-H_4te2p jsou ve srovnání s komplexy ligandu 1,4-H_4te2p stabilnější. Výjimku tvoří komplex s Cu(II), který má hodnotu $\log\beta_{011}$ zhruba o dva řády vyšší než je tomu u 1,8-H_4te2p. Vyšší stabilita je pravděpodobně dána uspořádáním pendantních fosfonátových skupin. V poloze 8 a 11 jsou dvě sekundární aminové skupiny, které umožňují vznik velice stabilního pětičlenného chelátového kruhu.

Slabší komplexy vytváří 1,4-H_4^{Me2}te2p. Důvodem je nižší bazicita aminových skupin kruhu. Ligand obsahuje pouze terciární aminové skupiny, které mají nižší bazicitu a také nižší koordinační schopnosti než sekundární aminové skupiny. Je známo, že čím je vyšší bazicita aminových skupin, tím je výsledný komplex stabilnější.[30]

Nejslabší komplexy ze studovaných ligandů vytváří 1,8-H_2^{Et2}te2p. Příčinou je opět nízká bazicita aminových skupin, neboť fosfonové monoesterové skupiny výrazně snižují elektronovou hustotu na blízkých atomech dusíku kruhu.

Z Tab. 3 je také patrné, že většina komplexů ligandů obsahující pendantní fosfonátové skupiny dosahuje vyšších hodnot konstant stability než jejich analoga s pendantními acetátovými skupinami. Důvodem je opět nižší bazicita aminových skupin nesoucích karboxylovou skupinu.

Všechny výše uvedené ligandy vytváří nejstabilnější komplexy s ionty Cu(II), což je v souladu s Irving-Williamsovou řadou. Dalším důvodem je vhodná velikost čtrnáctičlenných makrocyklů pro ionty Cu(II).[1, 14, 31] Fosfonátové ligandy jsou výrazně selektivnější pro vázání iontů Cu(II) než ligandy s pendantními acetátovými skupinami.

3 Závěr

Porovnáním hodnot odpovídajících si pK_a jednotlivých ligandů je zřejmé, že acidobazické vlastnosti studovaných ligandů se podobají vlastnostem strukturně příbuzných ligandů. Výrazně nižší pK_3 u 1,8-H_2^{Et2}te2p je vysvětlena přítomností fosfonové monoesterové skupiny. Rozdíly v hodnotách pK_1 a pK_2 již nejsou tak výrazné.

Podle očekávání tvoří 1,4-H_4te2p a 1,4-H_4^{Me2}te2p stabilní komplexy, zvláště pak s Cu(II). Konstanty obou těchto ligandů dosahují hodnot srovnatelných s hodnotami pro 1,8-H_4te2p. Nejslabší komplexy ze studovaných ligandů tvoří 1,8-H_2^{Et2}te2p.

Stabilita komplexů všech studovaných ligandů sleduje Irving-Williamsovou řadu, hodnoty konstant se tedy mění v pořadí Co(II) < Ni(II) < Cu(II) > Zn(II).

[1] X. Liang, P. J. Sadler: *Chem. Soc. Rev.*, **2004**, 33, 246

[2] D. Parker in *Comprehensive Supramolecular Chemistry*, Vol. 10, J. M. Lehn (ed.), Pergamon, **1996**, 487–536

[3] D. E. Reichert, C. J. Anderson, M. J. Welch: *Chem. Ind.*, **1998**, 730

[4] S. M. Okarvi: *Eur. J. Nucl. Med*, **2001**, 28, 929

[5] H. Lundqvist, V. Tolmachev: *Biopolymers*, **2002**, 66, 381

[6] D. Parker: *Chem. Soc. Rev.*, **1990**, 19, 271

[7] J. Zweit: *Phys. Med. Biol.*, **1996**, 41, 1905

[8] L. Yuanfang, W. Chuanchu: *Pure Appl. Chem.*, **1991**, 63, 427

[9] S. Liu, D. S. Edwards: *Bioconjugate Chem.*, **2001**, 12, 7

[10] P. J. Blower, J. S. Lewis, J. Zweit: *Nucl. Med. Biol.*, **1996**, 23, 957

[11] S. S. Jurisson, J. D. Lydon: *Chem. Rev.*, **1999**, 99, 2205

[12] D. E. Reichert, J. S. Lewis, C. J. Anderson: *Coord. Chem. Rev.*, **1999**, 184, 3

[13] J. J. Christensen, D. J. Eatough, R. M. Izatt: *Chem. Rev.*, **1974**, 74, 351

[14] a) S. F. Lincoln: *Coord. Chem. Rev.*, **1997**, 166, 255; b) K. P. Wainwright: *Coord. Chem. Rev.*, **1997**, 166, 35; c) M. Meyer, V. Dahaoui-Gindrey, C. Lecomte, R. Guilard: *Coord. Chem. Rev.*, **1998**, 178–180, 1313; d) L. F. Lindoy: *Adv. Inorg. Chem.*, **1998**, 45, 75

[15] D. Parker: *Chem. Br.*, **1994**, 818

[16] A. D. Sherry: *J. Alloys Compd.*, **1997**, 249, 153

[17] A. E. Martell, R. M. Smith: *Critical Stability Constants*, Vol. 1–6, Plenum Press, New York, **1974–1989**; *NIST Standard Reference Databáze 46 (Critically Selected Stability Constants of Metal Complexes), Version 7.0*, **2003**

[18] a) I. Belskii, Y. M. Polikarpov, M. I. Kabachnik: *Usp. Khim.*, **1992**, 61, 415; b) I. Lukeš, J. Kotek, P. Vojtíšek, P. Hermann: *Coord. Chem. Rev.*, **2001**, 216–217, 287

[19] J. Kotek, P. Vojtíšek, I. Císařová, P. Hermann, P. Jurečka, J. Rohovec, I. Lukeš: *Collect. Czech. Chem. Commun*, **2000**, 65, 1289

[20] H. Mollier, M. Vincens, M. Vidal, R. Pasqualini, M. Duet: *Bull. Soc. Chim. Fr.*, **1991**, 128, 787

[21] R. J. Motekaitis, B. E. Rogers, D. E. Reichert, A. E. Martell, M. J. Welch: *Inorg. Chem.*, **1996**, 35, 3821

[22] R. Delgado, J. J. R. Fraústo da Silva: *Talanta*, **1982**, 29, 815

[23] R. Delgado, L. C. Siegfried, T. A. Kaden: *Helv. Chim. Acta*, **1990**, 73, 140

[24] a) J. Rohovec, M. Kývala, P. Vojtíšek, P. Hermann, I. Lukeš: *Eur. J. Inorg. Chem.*, **2000**, 195; b) R. D. Hancock, R. J. Moitekaitis, J. Mashishi, I. Cukrowski, J. H. Reibenspies, A. E. Martell: *J. Chem. Soc., Perkin Trans. II*, **1996**, 1925

[25] a) T. Kiss, I. Lázár, P. Kafarski: *Metal-Based Drugs 1*, **1994**, 247; b) T. Kiss, I. Lázár in *Aminophosphonic and Aminophosphinic Acids. Chemistry and Biological Activity*, V. P. Kukhar, H. R. Hudson (eds.), Wiley, New York, **2000**, 285–326

[26] J. Rohovec, I. Lukeš, P. Vojtíšek, I. Císařová, P. Hermann: *J. Chem. Soc., Dalton Trans.*, **1996**, 2685

[27] J. Kotek: *Diplomová práce*, katedra anorganické chemie PřF UK, **1999**

[28] S. Chaves, R. Delgado, J. J. R. Fraústo Da Silva: *Talanta*, **1992**, 39, 249

[29] S. A. Pisareva, F. I. Belskii, T. Y. Medved, M. I. Kabachnik: *Izv. Akad. Nauk SSSR, Ser. Khim.*, **1987**, 413

[30] M. Lukáš, P. Vojtíšek, P. Hermann, J. Rohovec, I. Lukeš: *Synth. Commun.*, **2002**, 32, 79

[31] A. E. Martell, R. D. Hancock: *Metal Complexes in Aqueous Solutions*, Plenum Press, New York, **1996**

Thermodynamic, kinetic and solid-state study of divalent metal complexes of 1,4,8,11-tetraazacyclotetradecane (cyclam) bearing two *trans* (1,8-)methylphosphonic acid pendant arms†

Ivona Svobodová,[a] Přemysl Lubal,*[a] Jan Plutnar,[b] Jana Havlíčková,[b] Jan Kotek,[b] Petr Hermann*[b] and Ivan Lukeš[b]

Received 3rd March 2006, Accepted 14th September 2006
First published as an Advance Article on the web 22nd September 2006
DOI: 10.1039/b603251f

Divalent metal complexes of macrocyclic ligand 1,4,8,11-tetraazacyclotetradecane-1,8-bis(methylphosphonic acid)) (1,8-H_4te2p, H_4L) were investigated in solution and in the solid state. The majority of transition-metal ions form thermodynamically very stable complexes as a consequence of high affinity for the nitrogen atoms of the ring. On the other hand, complexes with Mn^{2+}, Pb^{2+} and alkaline earth ions interacting mainly with phosphonate oxygen atoms are much weaker than those of transition-metal ions and are formed only at higher pH. The same tendency is seen in the solid state. Zinc(II) ion in the octahedral *trans*-O,O-[$Zn(H_2L)$] complex is fully encapsulated within the macrocycle (N_4O_2 coordination mode with protonated phosphonate oxygen atoms). The polymeric $\{[Pb(H_2L)(H_2O)_2]\cdot 6H_2O\}_n$ complex has double-protonated secondary amino groups and the central atom is bound only to the phosphonate oxygen atoms. The phosphonate moieties bridge lead atoms creating a 3D-polymeric network. The $[\{(H_2O)_5Mn\}_2(\mu\text{-}H_2L)](H_2L)\cdot 21H_2O$ complex contains two pentaaquamanganese(II) moieties bridged by a ligand molecule protonated on two nitrogen atoms. In the complex cation, oxygen atoms of the phosphonate groups on the opposite sites of the ring occupy one coordination site of each metal ion. The second ligand molecule is diprotonated and balances the positive charge of the complex cation. Complexation of zinc(II) and cadmium(II) by the ligand shows large differences in reactivity of differently protonated ligand species similarly to other cyclam-like complexes. Acid-assisted dissociations of metal(II) complexes occur predominantly through triprotonated species $[M(H_3L)]^+$ and take place at pH < 5 (Zn^{2+}) and pH < 6 (Cd^{2+}).

Introduction

Investigations of highly thermodynamically stable and kinetically inert complexes (often formed by macrocyclic ligands)[1-5] have been stimulated by their applications in several areas, such as the contrast agents (CA) in magnetic resonance imaging (MRI),[6-9] for labelling of biomolecules with metal radioisotopes for both diagnostic and therapeutic purposes[10-14] or for luminescence optical imaging utilizing some lanthanide(III) ions which may be used for determination of a physiological status of tissues (healthy/diseased, change in pH or concentration of ions or metabolites *etc.*).[15,16] In the above medicinal utilizations, the harmful metal ion or radioisotope must not be deposited anywhere in body and the complex must be eliminated off unchanged from body.

In radiotherapy or diagnosis utilizing radioisotopes several elements are widely used, nowadays mostly technetium, iodine and fluorine. However, metal radioisotopes offer some advantages as they exhibit a wide range of physical properties (type of emitted particles, particle energy). Some of such metal radioisotopes (*e.g.* isotopes of Ga, In, Y and lanthanides) are routinely used in medicine as some suitable ligands for them have been found.[10-14] However, there is still a high demand to find more convenient ligands for these and other metal radioisotopes. The other metal radioisotopes include also clinically used Cu isotopes[17] (mostly β-emittors) or less common Bi, Pb and Tl isotopes[18] (α-emittors) having a great therapeutical potential but with almost no available suitable ligands. Such investigations are a living field of modern coordination chemistry.

As mentioned above, these metal complexes may be useful in medicine (in MRI and nuclear medicine or for luminescence imaging) if such complexes are highly stable under physiological conditions. Therefore, the complex with the particular metal ion must be thermodynamically stable and the ligand as selective as possible in a class of competing metal ions. However, it is now commonly recognized that kinetic inertness to dissociation of such complexes is also very important and is usually decisive for stability *in vivo*. Use of metal radioisotopes has raised another requirement—very fast complexation of short-living radioisotopes to enable to use of the isotopes in the kit form in hospitals.

[a]*Department of Analytical Chemistry, Masarykova universita (Masaryk University), Kotlářská 2, Brno, 611 37, Czech Republic. E-mail: lubal@chemi.muni.cz; Fax: +420-54949-2494; Tel: +420-54949-5637*

[b]*Department of Inorganic Chemistry, Universita Karlova (Charles University), Hlavova 2030, Prague 2, 128 40, Czech Republic. E-mail: petrh@natur.cuni.cz; Fax: +420-22195-1253; Tel: +420-22195-1263*

† Electronic supplementary information (ESI) available: Figures of speciation in some M^{2+}–H_4L, H^+–H_4L and M^{2+}–OH systems, crystal packing in structure of the Zn(II) and Mn(II) complexes, disorder simulation in structure of the Mn(II) complex, figure showing crystal structure of H_4L, examples of dependence of experimental $^fk_{obs}$ on c_{Zn} or c_{Cd}, tables with kinetic experimental data. See DOI: 10.1039/b603251f

From the viewpoint of thermodynamic stability and dissociation inertness, the macrocyclic ligands are more suitable for utilization of their metal complexes in medicine than the open-chain chelators. However, they often exhibit very slow complex formation kinetics in contrast to fast complexation with open-chain ligands (*e.g.* H_5dtpa and its derivatives). Macrocyclic ligands are mostly derivatives of two parent compounds—H_4dota and H_4teta (Scheme 1), derived from well-known cyclic amines, 1,4,7,10-tetraazacyclododecane (cyclen) and 1,4,8,11-tetraazacyclotetradecane (cyclam). H_4dota forms stable complexes with a number of common metal ions and is suitable for most of them, but preferable for lanthanide(III) ions requiring high coordination numbers.[1-5] H_4teta is more appropriate for transition-metal ions as a larger ring allows planar coordination of all nitrogen atoms.[1-5] However, such octadentate ligands do not usually utilize all donor atoms for binding to transition-metal ions in mononuclear species and they form polynuclear complexes.

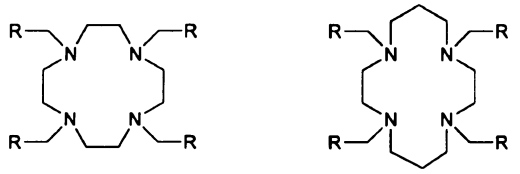

H_4dota H_8dotp H_4dotp^{Ph} H_4dotp^{H} R=CO_2H $P(O)(OH)_2$ P(Ph)(O)(OH) P(H)(O)(OH) H_4teta H_8tetp H_4tetp^{Ph}

Scheme 1

Many cyclen and cyclam phosphorus acid derivatives (mostly phosphonic acids H_8dotp and H_8tetp, Scheme 1) and their complexes have been investigated.[19-21] The phosphonic acid ligands are generally highly basic and, therefore, their complexes show a high thermodynamic stability.[19-26] Stability constants of the complexes of less basic phosphinic acid derivatives (*e.g.* H_4dotp^R and H_4tetp^R, Scheme 1) are lower but usually comparable with those of complexes of H_4dota and H_4teta.[27-29]

Some time ago, we have started investigations of ligands containing fewer phosphorus acid arms as such hexadentate ligands are more suitable for octahedral coordination to the transition-metal ions. Therefore, we decided to synthesize[22] 1,8-bis(phosphonic acid) derivatives of cyclam, namely 1,8-H_4te2p and 1,8-H_4te2pMe_2 (Scheme 2), having just six coordinating sites. The presence of phosphonic acid groups also overcomes the undesirable formation of the inner lactam described for an acetate analogue.[30] The *cis*- and *trans*-isomers of nickel(II)[31] and cobalt(III)[32] complexes of 1,8-H_4te2p (H_4L) were isolated in several differently protonated forms even such as $[Ni(H_4L)]^{2+}$, where the

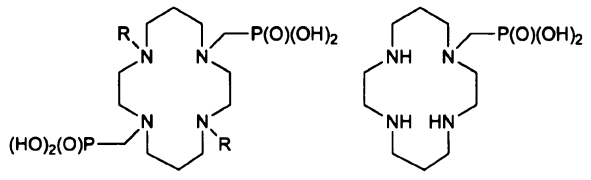

R=H 1,8-H_4te2p R=Me 1,8-H_4te2pMe_2 H_2te1p

Scheme 2

phosphonic groups are fully protonated and are coordinated only through the phosphoryl oxygen atom.[31] Such coordination was observed for the first time in the solid state. With copper(II), two extremely stable isomeric forms of $[Cu(H_2L)]$ were isolated.[33] The low-temperature kinetic isomer is five-coordinated with one phosphonic acid pendant arm uncoordinated. It isomerizes on heating to the thermodynamic octahedral isomer with *trans* arrangement of phosphonic acid moieties. As the complexes were intended as models for more sophisticated complexes possibly useful in nuclear medicine, very promising results were obtained from investigation of acid-assisted decomplexation.[33] The octahedral complex is one of the most kinetically inert complexes of copper(II). For both isomers, the slow decomposition may be a consequence of an overall positive charge of complex species on the full protonation of non-coordinated phosphonate oxygen atoms.[33] We proved that the complexation of copper(II) by the ligand is highly selective and we employed the property in an efficient analytical determination of copper.[34,35] The results show that 1,8-H_4te2p is one of the ligands most suitable for copper(II) complexation.

As the copper radioisotopes are produced by irradiation of parent nickel or zinc isotopes,[13] nickel(II) or zinc(II) ions are the most common chemical impurities in commercial sources of copper radioisotopes. For this reason, special selectivity for copper(II) complexation over the zinc(II) or nickel(II) binding is required.

In our previous studies, we focused on complexing behaviour of 1,8-H_4te2p with transition-metal ions (Cu^{2+}, Ni^{2+}, Co^{3+}).[31-35] Here, we report on the thermodynamic studies of 1,8-H_4te2p complexes with divalent transition-metal ions as well as with alkaline-earth ions. Three new crystal structures of the complexes are reported. In addition, we report on the formation and dissociation kinetics of zinc(II) and cadmium(II) complexes of the title ligand.

Experimental

Materials

The ligand, 1,8-H_4te2p·$4H_2O$ (H_4L·$4H_2O$), was synthesized by the method described elsewhere.[22] Analytical grade chemicals were purchased from Lachema (Czech Republic), Fluka or Merck and were used as received. For potentiometric titrations, metal nitrates or $MnSO_4$·$4H_2O$ (recrystallized from deionized water) were used and their stock solutions were standardized by titration with Na_2H_2edta according to the recommended procedure.[36] The stock solution of nitric acid (~0.03 mol dm^{-3}) was prepared from recrystallized KNO_3 on ion-exchange resin (Dowex 50). Diluted HNO_3 obtained by this way is more pure than that prepared from conc. HNO_3 as the concentrated acid contains traces of NO_x. Carbonate-free KOH stock solution (~0.2 mol dm^{-3}) was prepared from potassium metal (Aldrich) under argon atmosphere. The hydroxide solution was standardized against potassium hydrogen phthalate and the HNO_3 solution against the ~0.2 mol dm^{-3} KOH solution. The analytical grade chemicals employed in the kinetic studies were purchased from Lachema ($ZnCl_2$, $CdCl_2$·$6H_2O$, KOH, CH_3COOH) and Fluka (2-morpholine-ethanesulfonic acid, MES). The indicators bromocresol green (Lachema), bromocresol purple (Merck) and 4-(2-pyridylazo)resorcinol (PAR, Lachema) were of the highest available purity. The freshly prepared solutions of $CdCl_2$ and $ZnCl_2$

were standardized chelatometrically at pH ~9.2 (ammonia buffer) against Eriochrom black T.

Potentiometric titrations

The equilibria in ligand : metal systems with all metal ions except for Co^{2+} and Ni^{2+} were established in the course of minutes in each titration point and, thus, they could be studied by conventional titrations. The titrations were carried out in a thermostatted vessel at 25.0 ± 0.1 °C, at constant ionic strength $I(KNO_3)$ = 0.1 mol dm^{-3}, using a PHM 240 pH-meter, a 2 ml ABU 900 automatic piston burette and a GK 2401B combined glass electrode (all Radiometer). The ligand concentration in the titration vessel was *ca.* 0.004 mol dm^{-3}. The ligand-to-metal ratio was 1 : 1 in all cases. The initial volume was *ca.* 5 ml. The measurements were taken with a HNO_3 excess added to the mixture. The mixtures were titrated with the stock KOH solution in the region of $-\log[H^+] = 1.6–12.0$. Titrations for each system were carried out at least four times. Each titration consisted of *ca.* 40 points. Inert atmosphere was provided by constant passage of argon saturated with water vapour. The complexation reaction was too slow to be followed by standard titrations for systems with Co^{2+} and Ni^{2+}. These systems were studied by the "out-of-cell" method. Each titration consisted of *ca.* 25 solutions (two parallel titrations), each solution was mixed separately in the test tube (each sample volume *ca.* 1 ml) and an appropriate amount of the KOH solution was added to each test tube to simulate the common titration. The tubes were tightly closed and left to equilibrate for two days (Co^{2+}) or three weeks (Ni^{2+}). These equilibration times were determined in separate preliminary experiments. Then, the potential at each titration point (tube) was determined with freshly calibrated electrode.

The constants with their standard deviations were calculated using the OPIUM program package.[37] The program minimises the criterion of the generalised least-squares method using the calibration function given in eqn (1).

$$E = E_0 + S\log[H^+] + j_1[H^+] + j_2K_w/[H^+] \quad (1)$$

The term E_0 contains the standard potentials of the electrodes used and the contributions of inert ions to the liquid-junction potential. The term S corresponds to the Nernstian slope and the terms $j_1[H^+]$ and $j_2K_w/[H^+] = j_2 \times [OH^-]$ are contributions of the H^+ and OH^- ions to the liquid-junction potential. It is clear that j_1 and j_2 cause a deviation from a linear dependence of E and $-\log[H^+]$ only in strongly acidic and alkaline solutions. The calibration parameters were determined from titration of the standard HNO_3 with the standard KOH solutions before and after every titration of the ligand/metal ion system to give calibration–titration pairs used for calculations of stability constants. The concentration dissociation constants K_a of 1,8-H_4te2p (H_4L) were taken from the literature.[22] The stability constants β_{hlm} are defined as $\beta_{hlm} = [H_hL_lM_m]/([H]^h[L]^l[M]^m)$. The water ion product pK_w taken for calculations was 13.78. Stability constants of metal hydroxo complexes included in the calculations were taken from literature.[38–40]

Kinetic measurements

All experiments were made at a temperature 25.0 ± 0.2 °C. The ionic strength 0.1 mol dm^{-3} was maintained with KCl. The final pH of the buffered solution was checked by a pH-meter calibrated with standard buffers.

The formation kinetics of Cd^{2+} and Zn^{2+} complexes were followed under pseudo-first-order conditions ($c(MCl_2) = (1–10) \times 10^{-3}$ mol dm^{-3}, $c(H_4L) = 1 \times 10^{-4}$ mol dm^{-3}) in the pH (pH-meter calibrated with standard buffers) range 3.7–6.8 (Zn^{2+}) and 4.6–7.0 (Cd^{2+}); the indicator technique was used for detection of the reaction course.[41] The formation kinetics of the Cu^{2+} complex was followed in the pH range 5.0–7.0 analogously to a published procedure (stopped-flow measurements).[33] The reactions were performed in slightly buffered solution (0.005 mol dm^{-3} potassium acetate/acetic acid or MES acid/K^+-salt buffers) and the 2×10^{-5} mol dm^{-3} solution of indicator (bromocresol green (pH < 5.2) or bromocresol purple (pH > 5.2)) was used for visualization.

The dissociation kinetics of $[Zn(L)]^{2-}$ and $[Cd(L)]^{2-}$ complexes ($c = 1 \times 10^{-3}$ mol dm^{-3}) were measured in the pH range 3.7–4.8 (zinc(II) complex) and 4.5–6.1 (cadmium(II) complex) and in I = 0.1 mol dm^{-3}. The reactions were performed in buffered solution (0.05 mol dm^{-3} potassium acetate/acetic acid or MES acid/K^+-salt buffers). For both complexes, Cu^{2+} ion ($c(CuCl_2) = 1 \times 10^{-3}$ mol dm^{-3}, λ_{max} = 310 nm) was used as a ligand scavenger. For the $[Zn(L)]^{2-}$ complex, 4-(2-pyridylazo)resorcinol (PAR) ($c(PAR) = 2 \times 10^{-5}$ mol dm^{-3}, λ_{max} = 498 nm) was also utilized as a zinc(II) scavenger. It was verified (by checking of formation kinetics under our experimental conditions) that the visualisation reaction between the ligand or the metal ion and their scavengers was much faster than dissociation reaction of the studied complexes (for complexation kinetics of Cu^{2+} ion with H_4L, see also ref. 33). Dissociation kinetics was performed at different copper(II) concentrations to verify a direct transchelation reaction. No dependence of k_{obs} on c_{Cu} was observed (Table S5, ESI†). It confirms that complex dissociation is the rate-determining step followed by fast complexation with the scavenger.[42] Therefore, the transchelation can be neglected in further treatment of the experimental data.

The kinetic measurements were carried out on diode-array spectrophotometer HP 8453A (Hewlett Packard, USA) for slow kinetics ($10\tau_{1/2} > 10$ min) and on a Bio Sequential SX-17 stopped-flow spectrometer (Applied Photophysics, UK) for fast kinetics ($10\tau_{1/2} < 10$ min). The measured values of absorbance were corrected for the background analytical signal. Values of k_{obs} were obtained from experimental data by HP software and Excel[43] software with identical results. The dependence of k_{obs} on proton concentration were treated with Excel software.[43]

Preparation of single crystals

***trans*-O,O-[Zn(H_2L)].** A solution of $H_4L \cdot 4H_2O$ (50 mg, 0.11 mmol) in water (5 ml) was mixed with a solution of $Zn(OAc)_2 \cdot 2H_2O$ (24 mg, 0.11 mmol) in water (5 ml) and the mixture was sealed in a vial. The solution was heated to *ca.* 90 °C and held at this temperature overnight. Small colourless prisms of the product suitable for X-ray structure determination were formed on the walls of the vial. Yield ~70%.

$[\{(H_2O)_5Mn\}_2(\mu\text{-}H_2L)](H_2L) \cdot 21H_2O$. The ligand hydrate (50 mg, 0.11 mmol) and $MnCO_3$ (12.6 mg, 0.11 mmol) were added to water (5 ml) and refluxed under argon for 72 h (until $MnCO_3$ completely dissolves). The light yellow solution was then filtered and concentrated under vacuum to *ca.* 1 ml; pH of the

solution was *ca.* 5.5. On standing for several days, light yellow single crystals of the product appeared. Yield ~30%.

$[Pb(H_2L)(H_2O)_2]\cdot 6H_2O$. A solution of $H_4L\cdot 4H_2O$ (50 mg, 0.11 mmol) in water (5 ml) was mixed with a solution of $Pb(OAc)_2\cdot 3H_2O$ (39 mg, 0.11 mmol) in water (5 ml); pH of the solution was *ca.* 5. The solution was then evaporated under vacuum and the white residue was redissolved in water (1.5 ml). Colorless prisms of the product suitable for X-ray structure determination were formed on standing over several days. Yield ~35%.

Crystallography

Selected crystals were quickly transferred from the mother-liquor into Fluorolub oil, mounted on glass fibres in random orientation and cooled to 150(1) K. Diffraction data were collected using a Nonius Kappa CCD diffractometer (Enraf-Nonius) at 150(1) K (Cryostream Cooler, Oxford Cryosytem) using Mo-Kα radiation ($\lambda = 0.71073$ Å) and analyzed using the HKL program package.[44] The structures were solved by direct methods and refined by full-matrix least-squares techniques (SIR92 (ref. 45) and SHELXL97 (ref. 46)). Scattering factors for neutral atoms used were included in the SHELXL97 program. Table 1 gives pertinent crystallographic data.

In the structure of *trans*-O,O-$[Zn(H_2L)]$, the asymmetric unit consists of two independent halves of the complex molecule. Zinc atoms are located on the inversion centres. All non-hydrogen atoms were refined anisotropically. The hydrogen atoms were located in the electron density difference map. Nevertheless, hydrogens attached to carbon atoms were fixed in theoretical positions. Hydrogen atoms bound to nitrogen and oxygen atoms were refined isotropically.

In the structure of $\{[Pb(H_2L)(H_2O)_2]\cdot 6H_2O\}_n$, the metal ion and two halves of the macrocyclic ligand form the asymmetric unit. All non-hydrogen atoms except those belonging to two co-crystallized water molecules were refined anisotropically. All hydrogen atoms attached to carbon, nitrogen or coordinated oxygen atoms were located in the electron difference map; however, they were fixed in theoretical or original positions with thermal parameters $U_{eq}(H) = 1.2U_{eq}(C)$ or $1.3U_{eq}(N,O)$ as the free refinement led to unrealistic bond lengths. Some hydrogen atoms belonging to co-crystallized water molecules were also found and were treated using AFIX 3 instruction and $U_{eq}(H) = 1.3U_{eq}(O)$. Two oxygen atoms of water molecules were found disordered in several positions, and they were refined isotropically. Overall, the quality of the diffraction data was rather poor, probably due to a presence of several small crystallites on the main single crystal. Therefore, no successful absorption correction could be applied, which lead to a relatively big peak-and-hole difference (6.6 and −3.2 e Å^{-3}); they are located very close to the lead atom (0.81 and 0.68 Å, respectively).

The independent unit of $[\{(H_2O)_5Mn\}_2(\mu\text{-}H_2L)](H_2L)\cdot 21H_2O$ consists of the pentaaquamanganese(II) moiety coordinated by one oxygen atom of the pendant phosphonate belonging to one half of the ligand molecule (there is a centre of symmetry lying inside the macrocycle cavity). The other independent half of molecule of the ligand is not coordinated and serves as a counter anion and the macrocyclic part of this uncoordinated ligand molecule is highly disordered. This disorder was best described by

Table 1 Experimental and refinement data for the X-ray diffraction studies

Parameter	*trans*-O,O-$[Zn(H_2L)]$	$[Pb(H_2L)(H_2O)_2]\cdot 6H_2O$	$[\{(H_2O)_5Mn\}_2(\mu\text{-}H_2L)](H_2L)\cdot 21H_2O$
Empirical formula	$C_{12}H_{28}N_4O_6P_2Zn$	$C_{12}H_{44}N_4O_{14}P_2Pb$	$C_{24}H_{118}Mn_2N_8O_{43}P_4$
M_r	451.69	737.64	1441.02
T/K	150(1)	150(1)	150(1)
Crystal dimensions/mm	0.20 × 0.13 × 0.10	0.40 × 0.20 × 0.13	0.20 × 0.13 × 0.10
Shape	Prism	Prism	Prism
Colour	Colourless	Colourless	Pale yellow
Crystal system	Triclinic	Triclinic	Triclinic
Space group	$P\bar{1}$ (no. 2)	$P\bar{1}$ (no. 2)	$P\bar{1}$ (no. 2)
a/Å	9.4638(7)	10.029(1)	9.7361(3)
b/Å	9.5509(6)	10.416(1)	12.2695(4)
c/Å	11.1074(8)	14.322(1)	14.0948(4)
α/°	89.068(4)	77.055(2)	87.808(2)
β/°	88.094(3)	73.698(2)	77.378(2)
γ/°	60.882(3)	71.776(2)	88.4157(13)
V/Å^3	876.61(11)	1348.6(2)	1641.51(9)
Z	2	2	1
D_c/g cm^{-3}	1.711	1.817	1.458
μ/mm^{-1}	1.622	6.444	0.584
$F(000)$	472	756	772
θ Range of data collection/°	3.05–27.53	3.29–27.65	2.96–27.51
Index ranges, hkl	−12 to 12, −12 to 12, −13 to 14	−12 to 13, −13 to 13, −18 to 18	−12 to 12, −15 to 15, −18 to 18
Reflections measured	3913	6088	7504
Reflections observed $[I > 2\sigma(I)]$	2973	5864	5560
Data, restraints, parameters	3913, 0, 341	6088, 0, 303	7504, 0, 406
Goodness-of-fit on F^2	1.039	1.159	1.040
R, R' indices $[I > 2\sigma(I)]^a$	0.0743, 0.0522	0.0473, 0.0453	0.0755, 0.0485
wR, wR' $[I \geq 2\sigma(I)]^a$	0.1405, 0.1265	0.1033, 0.1022	0.1224, 0.1080
Maximum shift/esd	0.001	0.001	0.007
$\Delta\rho_{max, min}$/e Å^{-3}	1.199, −0.829	6.576, −3.228	0.983, −0.903

[a] $w = 1/[\sigma^2(F_o^2) + (AP)^2 + BP]$, $P = (F_o^2 + 2F_c^2)/3$ (ref. 46) and R, $R' = \sum|F_o - F_c|/\sum|F_c|$; wR, $wR' = [\sum w(F_o^2 - F_c^2)^2/\sum w(F_o^2)^2]^{1/2}$ (ref. 46).

placing of part of macrocycle into two positions with occupancies approximately 63 : 37. However, both conformations are very similar (Fig. S5, ESI†). As some C–C distances became too long during a free refinement they were treated using DFIX command; however, it lead to very prolate thermal ellipsoids with large max./min. ratio of anisotropic displacement parameters (up to 8.5), indicating possibly a more complicated disorder. Additionally, 10 water molecules of crystallization were found in the independent unit and the 11th was best refined with half-occupancy. In the pentaaquamanganese(II) unit, one of the coordinated water molecules was found to be disordered in two positions and was refined isotropically with relative occupancies 77 : 23. Other non-hydrogen atoms were refined anisotropically. The hydrogen atoms belonging to the carbon or nitrogen atoms of the coordinating ligand molecule or to co-crystallized water molecules were located in electron difference map, but they were fixed in theoretical positions with thermal parameters $U_{eq}(H) = 1.2U_{eq}(C)$ or $1.3U_{eq}(N)$ or kept in the original geometry using AFIX 3 instruction with $U_{eq}(H) = 1.3U_{eq}(O)$; the free refinement lead to unrealistic bond lengths and values of thermal parameters. The hydrogen atoms of the disordered uncoordinated ligand molecule were fixed in theoretical positions using the same riding model.

CCDC reference numbers 600826–600828.

For crystallographic data in CIF or other electronic format see DOI: 10.1039/b603251f

Results and discussion

Thermodynamic stability of metal complexes

As expected, values of stability constants of alkaline earth metal ions are low (Table 2); nevertheless, differences in titration curves of the pure ligand and of ligand–M^{2+} systems are different (Fig. S1, ESI†) and the constants were determined with satisfactory precision. Complexation of the metal ions starts in slightly acid region (−log[H^+] 5–6) by formation of low-abundant (~20%) diprotonated H_2LM species (representative distribution diagrams for Mg^{2+} and Ca^{2+} systems are shown in Fig. S2, ESI†). Protons from the species (as well as from the free ligand) are removed only in highly alkaline solutions and, thus, the species with LM stoichiometry have a reasonable abundance only in the strong alkaline region (−log[H^+] >10 for Mg^{2+} and >12 for Ca^{2+}, Sr^{2+} and Ba^{2+}). It also corresponds to pK_a values related with deprotonations of the H_2LM and HLM species (Table 2, pK_a = 10.8–12.1). They are much higher than those corresponding to deprotonation(s) of the phosphonate moieties (pK_a = 5.36 (H_4L) and 6.78 (H_3L)) and lower than those assigned to deprotonations of $>NH_2^+$ groups (pK_a ~13.2 for the H_2L/HL species) of the free ligand. One can attribute deprotonations of the H_2LM and HLM species to the proton dissociations from secondary amino groups of the macrocycle. Thus, the metal ions would be bound only by oxygen atoms of the pendant groups in the double-protonated H_2LM species and coordination of nitrogen atoms can occur only in LM (and possibly also in HLM) species. Among alkaline earth ions, it is clearly seen that the ligand is selective for Mg^{2+} (unlike H_4teta) as a consequence of a higher affinity of phosphonates to the small hard cation.

Previously, we have proved[31,32,33] for Ni^{2+}, Co^{2+}/Co^{3+} and Cu^{2+} ions that only kinetic (*cis*-O,O or pentacoordinated, respectively) isomers are formed at room temperature and all nitrogen atoms are bound in these complexes. Therefore, *cis*-O,O arrangement is expected for the highly stable complexes (Table 2) of transition-metal ions (Co^{2+}, Ni^{2+}, Zn^{2+} and Cd^{2+}) formed during potentiometric titrations. Complexation starts in the acid solutions (Fig. 1 and S2, ESI†) and we assume coordination of the macrocyclic ring nitrogen atoms even in acid region. This is supported by values of pK_a corresponding to deprotonation of the H_2LM and HLM species (Table 2) as they are much lower than values corresponding to the last two proton dissociations from the free ligand and are more comparable with those for proton dissociations from phosphonate moieties of the free ligand. The acidity of H_2LM species is mostly higher (pK_a in the range 4.5–5.6) in comparison with that of the PO_3H^- moieties of the free ligand (5.36, 6.78) indicating coordination of the pendant group(s) as their acidity is increased due to the electron-withdrawing effect of the metal ion when bound. However, the acidity of the HLM species is lower (pK_a in the range 7.2–7.8) than that of the last PO_3H^- moiety in the free ligand (pK_a corresponding to this proton dissociation is 6.78). This effect can be attributed to a presence of an intramolecular hydrogen bond between coordinated pendant arms ($-PO_3^{2-}$ and $-PO_3H^-$) which is possible only in a *cis*-O,O

Table 2 Stability constants of metal ion complexes with 1,8-H_4te2p[a] (25 °C, I = 0.1 mol dm^{-3} KNO_3)

Equilibrium[b]	*hlm*	Mg^{2+}	Ca^{2+}	Sr^{2+}	Ba^{2+}	Mn^{2+}	Co^{2+}	Ni^{2+}	Cu^{2+}[c]	Zn^{2+}	Cd^{2+}	Pb^{2+}
		$\log\beta_{hlm}$										
M + L ⇌ ML	011	8.61(5)	5.26(3)	4.09(4)	3.90(13)	12.35(3)	19.28(6)	21.99(8)	25.40	20.35(4)	17.89(3)	14.96(3)
H + L + M ⇌ HML	111		16.93(6)		16.39(7)	21.22(4)	27.09(3)	29.30(5)	32.45	27.52(2)	25.45(1)	23.97(1)
2H + L + M ⇌ H_2ML	211	28.35(9)	28.43(5)	28.30(8)	28.01(11)		31.57(7)	34.07(3)	37.55	31.96(5)	31.04(2)	29.72(4)
3H + L + M ⇌ H_3ML	311					35.1(1)						
		pK_a										
H_2ML ⇌ HML + H			11.50		11.6		4.48	4.77	5.10	4.44	5.59	5.75
HML ⇌ ML + H			11.67		12.49	8.87	7.81	7.31	7.05	7.17	7.56	9.01
H_2ML ⇌ ML + 2H		19.74		24.21								
H_3ML ⇌ HML + 2H						13.9						

[a] Dissociation constants[22] of 1,8-H_4te2p = H_4L: pK_{HL} + pK_{H_3L} = 26.41; pK_{H_3L} = 6.78; pK_{H_4L} = 5.36; pK_{H_5L} = 1.15. [b] Charges are omitted for clarity. [c] Values for pentacoordinated complex; taken from ref. 33.

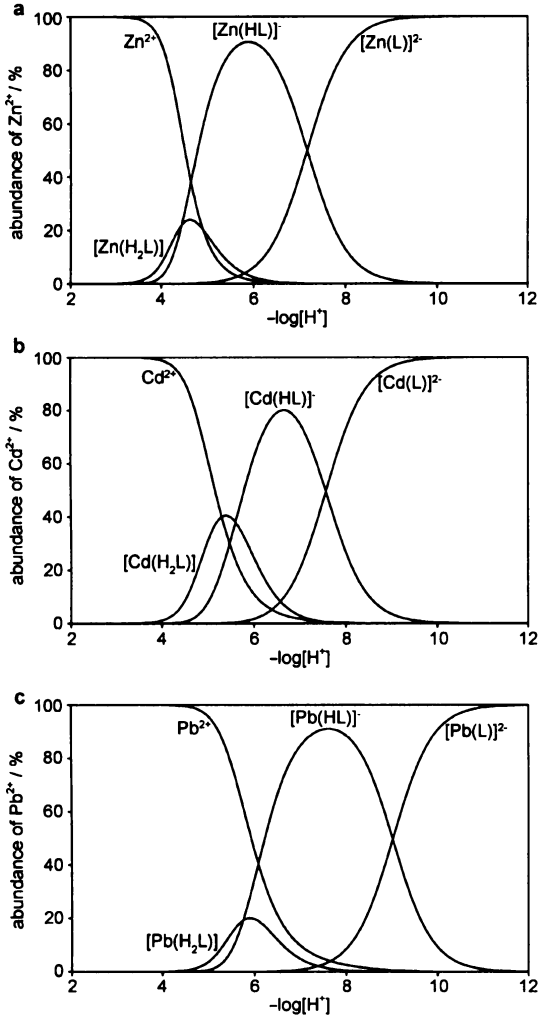

Fig. 1 Distribution diagrams of M^{2+}–1,8-H_4te2p systems ($c_M = c_L$ = 0.004 mol dm^{-3}); M = Zn (a), Cd (b) and Pb (c).

arrangement assumed for these species. Such a hydrogen bond would stabilize the last proton and it would lead to an increase in pK_a value assigned to the proton dissociation. A difference in pK_a values for the *cis*-O,O-[Co^{III}(HL)] complex (6.98) exhibiting much higher pK_a than its *trans*-O,O-[Co^{III}(HL)] isomer (2.97) has been explained by presence of the intramolecular hydrogen bond in the *cis* isomer.[32] The intramolecular hydrogen bond was found in the solid-state structures ot the *cis*-O,O-[Co^{III}(HL)][32] and *cis*-O,O-[Ni(H_2L)][31] complexes. In addition, acid–base titration of the prepared solid *cis*-O,O-[Ni(H_2L)] complex (employing a high kinetic inertness of the complex in acid solution) led to identical dissociation constants for the H_2LNi and HLNi species (4.78 and 7.35, respectively).[31] It is an indirect proof that structures of the complex in the solid state and the species present in solution under equilibrium conditions (this paper) should be identical. Therefore, we assume *cis* coordination of the pendant groups in the complexes of the transition-metal ions. On the other hand, Cu^{2+} forms at room temperature pentacoordinated species (N_4O coordination mode) and the corresponding pK_a value (7.05) was attributed to deprotonation of the uncoordinated phosphonate.[33]

A comparison of abundances of various forms of Zn^{2+} and Cd^{2+} complexes (relevant to kinetic studies, see below) is shown in Fig. 1. The highest stability was found for the copper(II) complex[33] (Table 3) and it reflects the usual Irving–Williams trend and optimal size of the fourteen-membered macrocyclic cavity for divalent copper.[17,47,48] The ligand is highly selective for Cu^{2+} (but less than cyclam itself) and the property has been explored in analytical determination of the ion in the presence of a range of competing ions.[34,35] In comparison with H_4teta, there are much larger differences in values of stability constants of 1,8-H_4te2p with most of the divalent metal ions studied.

The behaviour of divalent manganese and lead complexes is just on borderline. Both the metal ions have a higher affinity to harder oxygen donor atoms. In the H_2LM species, they should be bound to phosphonate moiety(ies) with double-protonated ring nitrogen atoms. This is supported by pK_a values corresponding to the HLM species (9.01 and 8.87 for Pb^{2+} and Mn^{2+}, respectively) and structure of the complexes isolated in the solid state (see below). The neutral solid complexes (having H_2LM stoichiometry) were isolated in the pH region where the protonated species are present. Binding of nitrogen atom(s) should be assumed in the ML species. Such behaviour is a consequence of the high basicity of the nitrogen atoms in the free ligand and a relatively high donor ability of the deprotonated phosphonate moiety(ies). Distribution diagrams for Pb^{2+} and Mn^{2+}–1,8-H_4te2p systems are shown in Fig. 1 and S2, ESI,† respectively.

Table 3 Comparison of stability constants ($\log \beta_{011}$) of metal complexes of 1,8-H_4te2p with those of related ligands

ion	1,8-H_4te2p	Cyclam[38]	H_2te1p[49]	H_8tetp[50]	H_4tetp^{Ph} [29]	H_4teta[51,52]
Mg^{2+}	8.61	—	5.39	—	—	1.97
Ca^{2+}	5.26	—	3.07	—	—	8.4
Sr^{2+}	4.09	—	—	—	—	5.82
Ba^{2+}	3.90	—	—	—	—	4.1
Mn^{2+}	12.35	—	11.81	10.8	—	11.3
Co^{2+}	19.28	14.3	—	—	—	16.6
Ni^{2+}	21.99	22.2	—	—	—	19.91
Cu^{2+}	25.40 (*pc*)[a 33] 26.50 (*trans*)[b 33]	28.1	27.3	26.6 25.99[53]	17.19	21.7
Zn^{2+}	20.35	15.2	21.07	17.6	9.79	16.40
Cd^{2+}	17.89	11.3	15.91	16.7	9.91	18.0
Pb^{2+}	14.96	10.9	—	15.5	—	14.3

[a] *pc* means kinetic pentacoordinated species. [b] Thermodynamic *trans*-O,O octahedral species.

To test the chemical model found by potentiometry we carried out some NMR measurements on magnesium(II)– and lead(II)–H_4L systems. Under conditions used for potentiometry (0.004 M, room temperature), only ^{31}P NMR spectra could be recorded. Unfortunately, in all tested pH values from 4 up, only rather broad nondiagnostic peaks were obtained. It is probably caused by some equilibria of coordinated–non-coordinated forms of the ligand and/or by equilibria between different conformation of the complexes if the ligand is fully bound. Unfortunately, no signal(s) for ^{207}Pb could be detected. At higher concentrations (0.01–0.1 M, to improve signal-to-noise ratio mainly for ^{207}Pb NMR), the ^{31}P NMR spectra above pH ~4 were again broad or gave more signals (probably the consequence of a presence of more isomeric species). More important, samples with the higher concentration of reactants precipitated at pH > 4.5–5 for Pb^{2+} and pH > 7 for Mg^{2+}. These partial NMR results indirectly prove probable presence of multiple microscopic equilibria and/or more isomers (at higher pH where ring nitrogen atoms are coordinated, *e.g.* as in the Zn^{2+}–cyclam system[54]) and, thus, coordination of nitrogen atoms at higher pH. Such a microscopic equilibria (possibly present only on NMR timescale) cannot be, principally, detected by normal potentiometry.

Zinc(II), lead(II) and manganese(II) complexes in the solid state

All single-crystals were obtained from solutions having pH 5–6 containing the protonated species (according to the distribution diagrams, see Fig. 1 and S2, ESI†). The colourless single crystals of *trans*-O,O-[Zn(H_2L)] complex were grown hydrothermally by heating an equimolar Zn^{2+}–1,8-H_4te2p mixture at 90 °C. Therefore, the thermodynamic *trans*-isomer was obtained. Single crystals of the $\{[Pb(H_2L)(H_2O)_2]\cdot 6H_2O\}_n$ and $[\{(H_2O)_5Mn\}_2(\mu\text{-}H_2L)](H_2L)\cdot 21H_2O$ complexes were obtained by a slow evaporation of their aqueous solutions. Overall H : L : M stoichiometry (number of protons) of the neutral complexes in the solid state corresponds well to distribution diagrams obtained from potentiometric studies; they were crystallized from solutions having pH where protonated species are present. However, such polymeric complexes are hardly expectable in solution and they should be formed only during crystallization.

***trans*-O,O-[Zn(H_2L)] complex.** The diffraction analysis revealed almost regular octahedral coordination sphere of Zn^{2+} cation with *trans* configuration of the pendant moieties (Fig. 2). In the crystal structure, two independent centrosymmetric complex molecules are present; however, the geometries of both molecules are almost the same and, thus, only one of them is shown in Fig. 2. Important distances and angles are given in Table 4. The cyclam ring exhibits the most stable ***trans*-III** arrangement.[55] The same configuration of the ring was found in the high-temperature isomers of the Ni^{2+} (ref. 31) Cu^{2+} (ref. 33) and Co^{3+} (ref. 32) complexes of 1,8-H_4te2p. At room temperature, the *cis* isomers are formed (see also above).[31,32] Unfortunately, we were unable to obtain reproducibly any complex with the expected *cis* arrangement in the solid state shortly after mixing and pH adjustment.

Good quality of crystal data allowed us to refine the positions of all hydrogen atoms. In each of the independent units, the acid hydrogen atoms are attached to uncoordinated oxygen atoms of pendant phosphonate O12 stabilizing the structure by strong intermolecular hydrogen bonding with unprotonated O13 oxygen atoms of the neighbouring molecule (d(O12–O13) = 2.55 Å for both independent molecules). Furthermore, the unprotonated oxygen atom O13 is involved in hydrogen binding to secondary amino group (N4, d(O13–N4) = 3.11 and 3.29 Å for the independent units). Such intermolecular hydrogen bond network connects the complex molecules in *yz* plane forming a layered structure (Fig. S3, ESI†). As a consequence of the hydrogen bond network, the complex is almost insoluble in water at neutral pH and dissolves only after deprotonation of phosphonate groups at alkaline pH. The octahedron around Zn^{2+} is more regular (bond lengths 2.11–2.15 Å and angles 86–94°; Table 4) compared with that in the X-ray crystal structure of [Zn(H_2teta)]·$4H_2O$.[56] The H_4teta complex represents the same ***trans*-III** conformation of the ring with two pendant acetate arms uncoordinated and its zinc(II) *trans*-N_4O_2 octahedron is more distorted with two longer Zn–N bonds (2.25 Å).

Table 4 Selected geometric parameters of the *trans*-O,O-[Zn(H_2L)] complex

	Molecule A	Molecule B
Zn1–N1	2.143(4)	2.153(4)
Zn1–N4	2.116(4)	2.111(4)
Zn1–O11	2.138(3)	2.155(3)
P1–O11	1.493(4)	1.496(4)
P1–O12	1.567(3)	1.573(3)
P1–O13	1.493(3)	1.490(3)
P1–C8	1.835(5)	1.829(6)
N1–Zn1–N4	86.1(2)	85.6(2)
N1–Zn1–N1[a]	180	180
N1–Zn1–N4[a]	93.9(2)	94.4(2)
N1–Zn1–O11	86.7(1)	85.9(1)
N1–Zn1–O11[a]	93.3(1)	94.1(1)
N4–Zn1–N4[a]	180	180
N4–Zn1–O11	92.3(2)	91.7(1)
N4–Zn1–O11[a]	87.7(2)	88.3(1)
O11–Zn1–O11[a]	180	180

[a] Equivalent atoms obtained through the centre of symmetry placed in the central zinc atom.

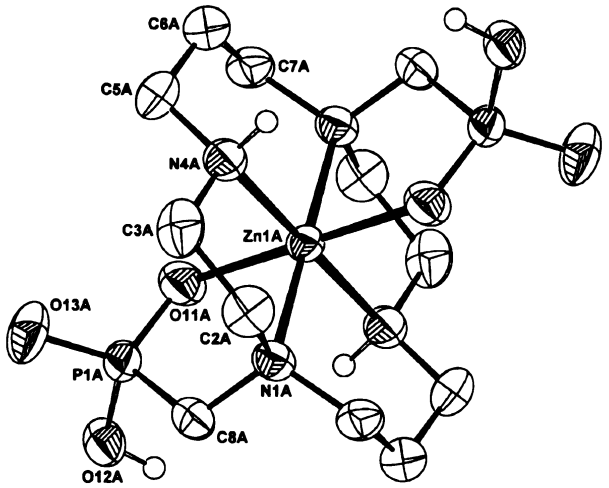

Fig. 2 Molecular structure of *trans*-O,O-[Zn(H_2L)] complex with atom numbering scheme. Hydrogen atoms attached to carbon atoms are omitted for clarity.

$\{[Pb(H_2L)(H_2O)_2]\cdot 6H_2O\}_n$ complex. The structure is shown in Fig. 3 and all important distances and angles are given in Table 5. The lead(II) ion is coordinated by five oxygen atoms, of which three belong to phosphonate groups and two to water molecules. The Pb–O length for one water molecule is rather long pointing to a very weak coordination (2.99 Å), the second water molecule is coordinated much closer to the metal ion (2.53 Å). The negatively charged phosphonate oxygen atom O11A forms the shortest bond (2.24 Å). The two neighbouring metal ions are connected *via* bridging O11B (the O11B–Pb and O11B–Pb# bond distances are 2.32 and 2.49 Å, respectively). The metal ions are separated by 3.93 Å, suggesting no direct metal–metal interaction. The central atom metal ion coordination sphere geometry is very irregular; it could be approximated as an octahedron with one missing vertex

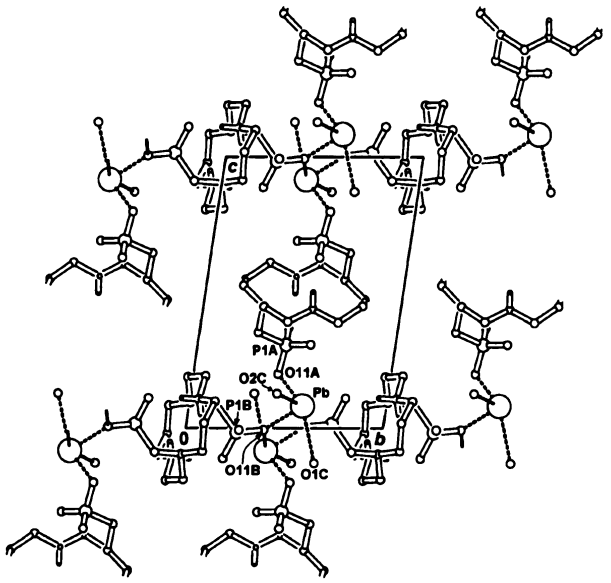

Fig. 3 The polymeric motif found in the solid-state structure of $\{[Pb(H_2L)(H_2O)_2]\cdot 6H_2O\}_n$ complex. The view down to *x* axis. Uncoordinated water molecules and hydrogen atoms attached to carbon atoms are omitted for clarity.

Table 5 Selected geometric parameters found in the structure of $\{[Pb(H_2L)(H_2O)_2]\cdot 6H_2O\}_n$

Pb–O11A	2.245(5)	O11A–Pb–O11B	81.2(2)
Pb–O11B	2.318(4)	O11A–Pb–O11B#	84.8(2)
Pb–O11B#	2.485(5)	O11A–Pb–O1C	151.4(2)
Pb–O1C	2.992(7)	O11A–Pb–O2C	86.4(2)
Pb–O2C	2.525(5)	O11B–Pb–O11B#	70.2(2)
Pb–Pb#	3.9306(5)	O11B–Pb–O1C	72.2(2)
O_4-plane-Pb[b]	−0.474(3)	O11B–Pb–O2C	81.3(2)
		O11B#–Pb–O1C	76.9(2)
P1A–O11A	1.552(5)	O11B#–Pb–O2C	151.2(2)
P1A–O12A	1.524(6)	O1C–Pb–O2C	99.1(2)
P1A–O13A	1.501(5)		
P1A–C8A	1.825(7)		
P1B–O11B	1.550(5)		
P1B–O12B	1.511(5)		
P1B–O13B	1.523(5)		
P1B–C8B	1.821(7)		

[a] Equivalent atoms obtained through the centre of symmetry placed in the middle between the lead atoms. [b] Distance of Pb^{2+} ion from the basal plane formed by O1C, O2C, O11A and O11B# atoms.

and lead atom lying below the basal O_4-plane (Table 5). The basal plane is formed by two water O1C and O2C oxygen atoms and by phosphonate O11A and O11B# oxygen atoms with O11B atom in the apical position. The neighbouring metal units share O11B and O11B# atoms in their basal and apical positions, respectively. The irregular arrangement clearly shows that the free electron pair on lead ion is stereochemically active. The macrocycle is not coordinated and the secondary amino groups are protonated, assuring electroneutrality of the system. The structure indicates that the complex with analogous protonation may be present as 211 species in solution confirming the results obtained by potentiometry (see above).

Coordination of nitrogen atom(s) in lead(II) complexes of (aminomethyl)phosphonic acids is rather rare and it was observed only in several compounds prepared mostly by hydrothermal synthesis.[57] The four-membered (P)–OPb_2O–(P) rings were found only in three compounds, namely in polymeric lead(II) (aminoalkyl)phosphonic acid complexes[57d,e,58] having similar structural parameters to those of our four-membered ring.

$[\{(H_2O)_5Mn\}_2(\mu\text{-}H_2L)](H_2L)\cdot 2H_2O$ complex. The secondary amino groups are protonated and no ring nitrogen atoms are coordinated, similarly to the lead(II) complex (see above). Each pentaaquamanganese(II) ion is bound to one oxygen atom of pendant phosphonate groups on the opposite sites of the cycle and, thus, the ligand bridges two manganese atoms forming the $[\{(H_2O)_5Mn\}_2(\mu\text{-}H_2L)]^{2+}$ cation (Fig. 4). The coordination geometry around Mn^{2+} is slightly distorted octahedron (Table 6).

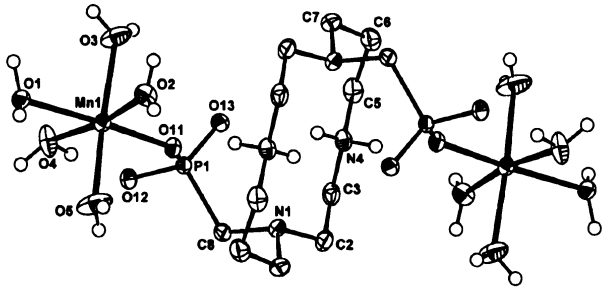

Fig. 4 Molecular structure of $[\{Mn(H_2O)_5\}_2(\mu\text{-}H_2L)]^{2+}$ cation with atom numbering scheme. Hydrogen atoms attached to carbon atoms are omitted for clarity.

Table 6 Selected geometric parameters found in the structure of $[\{(H_2O)_5Mn\}_2(\mu\text{-}H_2L)](H_2L)\cdot 2H_2O$

Mn–O11	2.123(2)	O11–Mn–O1	172.05(7)
Mn–O1	2.246(2)	O11–Mn–O2	99.00(7)
Mn–O2	2.146(2)	O11–Mn–O3	88.46(7)
Mn–O3	2.164(2)	O11–Mn–O4A#	89.35(8)
Mn–O4A#	2.199(3)	O11–Mn–O5	94.83(8)
Mn–O5	2.197(2)	O1–Mn–O2	88.92(7)
		O1–Mn–O3	91.73(7)
P1–O11	1.541(2)	O1–Mn–O4A#	82.70(7)
P1–O12	1.533(2)	O1–Mn–O5	86.36(8)
P1–O13	1.519(2)	O2–Mn–O3	83.97(8)
P1–C8	1.826(3)	O2–Mn–O4A#	170.06(9)
P2–O21	1.524(2)	O2–Mn–O5	85.77(9)
P2–O22	1.530(2)	O3–Mn–O4A#	92.91(10)
P2–O23	1.515(2)	O3–Mn–O5	169.60(10)
P2–C18	1.820(2)	O4A#–Mn–O5	98.97(11)

[a] The most abundant position of O4 atom (77%).

The dinuclear complex species lie in the direction of z axis. The electroneutrality of the crystal is assured by uncoordinated double-deprotonated ligand anion $(H_2L)^{2-}$, which is located in the cavities along y axis and serves as a counter anion (Fig. S4, ESI†). The skeleton of the anion is severely disordered (Fig. S5, ESI†) and, therefore, correct location of protons on the nitrogen atoms cannot be unambiguously determined; but protonation of secondary amino groups is expected to be analogous to the previous unit and is in accordance with the behaviour of the ligand in solution.[22] The free space in the packing accommodates solvate water molecules. Whole structure is stabilized by an extensive network of medium-to-strong hydrogen bonds between amino groups, coordinated water molecules, phosphonate oxygen atoms and solvate water molecules. Both macrocyclic units (of both coordinated and uncoordinated ligands) are in the same conformation found in most of the structures of cyclam derivatives with diprotonated ring.[4] It should be noted that the $[Mn(H_2O)_5(\text{oxygen donor})]^{2+}$ structure motif in the solid has been observed several times and no structure of manganese(II) complexes with (aminomethyl)phosphonate derivatives contains coordinated nitrogen atom(s) as result of CCDC search.[59] Only the manganese(II) complex of a macrocyclic phosphorus acid derivative is a polymeric $[Mn(H_6dotp)]$ complex (H_8dotp = 1,4,7,10-tetraazacyclododecane-1,4,7,10-tetrakis(methylphosphonic acid)) where the pendant arms are bound only through one oxygen atom of a monoprotonated phosphonate moiety and the ring is also protonated on two nitrogen atoms.[60]

Kinetics of formation of zinc(II) and cadmium(II) complexes

The formation of zinc(II) and cadmium(II) complexes is relatively slow at pH in the range 3.7–5 which makes it possible to follow the reaction using conventional UV-VIS spectroscopy. As there is no absorbing group or species, indirect indicator method (commonly employed in chemistry of macrocyclic ligands[41,42b,61]) was used to visualize course of the reactions. The method is simple but leads to somewhat less precise results compared with conventional direct methods.[62] At pH higher than 5, the stopped-flow technique was employed as the reactions are noticeably faster.

According to the distribution diagram of the free ligand, three differently protonated species, H_4L, H_3L^- and H_2L^{2-}, are present in an aqueous solution of the ligand in the pH region 3.7–7 (Fig. S6, ESI†). Therefore, each of those ligand species can take part in complexation reaction with Zn^{2+} or Cd^{2+} ions to form the final $[M(H_nL)]^{n-2}$ ($n = 0$–2) complexes and such particular reactions are characterized by corresponding second-order rate constants ${}^fk_{H_nL}$ ($n = 2$–4) as shown in Scheme 3.

The complex formation from the metal ion and the ligand can be considered as a second-order reaction with the rate law given in eqn (2):

$$v = {}^fk_2[L]_{tot}[M^{2+}]_{tot} \quad (2)$$

where $[L]_{tot}$ is total ligand concentration given by eqn (3) considering the ligand protonation constants β_n ($\beta_n \equiv \beta_{h10}$) as defined in the potentiometric section.

$$[L]_{tot} = [H_4L] + [H_3L^-] + [H_2L^{2-}] = (\beta_4[H^+]^4 + \beta_3[H^+]^3 + \beta_2[H^+]^2)[L^{4-}] = a_L[L^{4-}] \quad (3)$$

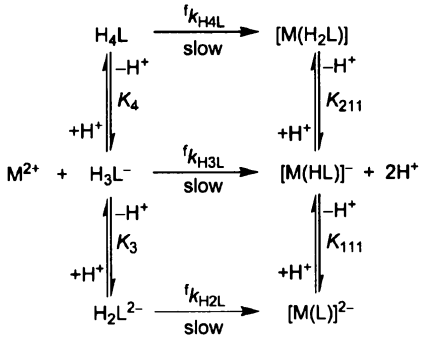

Scheme 3 Formation of 1,8-H_4te2p metal complexes (Cu^{2+}, Zn^{2+} and Cd^{2+}).

If the concentration of metal ion is much higher than the concentration of ligand, the eqn (2) could be rewritten into the pseudo-first order rate law given by eqn (4):

$$v = k_{obs}[L]_{tot} \quad (4)$$

where k_{obs} is the observed pseudo-first rate constant linearly dependent on the metal ion concentration defined by eqn (5).

$$k_{obs} = {}^fk_2[M^{2+}]_{tot} \quad (5)$$

The rate law developed from the general Scheme 1 is represented by eqn (6) (as in this case $[M^{2+}]_{tot} = [M^{2+}]$).

$$v = {}^fk_{H_4L}[H_4L][M^{2+}] + {}^fk_{H_3L}[H_3L^-][M^{2+}] + {}^fk_{H_2L}[H_2L^{2-}][M^{2+}] \quad (6)$$

Combining eqns (2), (3) and (6), one obtains eqn (7), which can be simplified to give eqn (8).

$${}^fk_2a_L[L^{4-}][M^{2+}] = {}^fk_{H_4L}\beta_4[H^+]^4[L^{4-}][M^{2+}] + {}^fk_{H_3L}\beta_3[H^+]^3[L^{4-}][M^{2+}] + {}^fk_{H_2L}\beta_2[H^+]^2[L^{4-}][M^{2+}] \quad (7)$$

$${}^fk_2a_L = {}^fk_{H_4L}\beta_4[H^+]^4 + {}^fk_{H_3L}\beta_3[H^+]^3 + {}^fk_{H_2L}\beta_2[H^+]^2 \quad (8)$$

Therefore, the dependence of the evaluated second-order rate constant on proton concentration can be expressed by eqn (9).

$${}^fk_2 = \frac{{}^fk_{H_4L}\beta_4[H^+]^4 + {}^fk_{H_3L}\beta_3[H^+]^3 + {}^fk_{H_2L}\beta_2[H^+]^2}{a_L} \quad (9)$$

At the first stage, it was proved that the collected data correspond to a first-order process with respect to the metal ion. It was shown that the dependence of the pseudo-first order rate constant (measured at constant pH) is a linear function of metal ion concentration (according to eqn (5)). Examples of the experimental data and their analysis are available in the ESI.† Therefore, a formation of complexes with higher metal-to-ligand ratio (*e.g.* M_2L) can be excluded. In the next step, the obtained second-order formation rate constants ${}^fk_2$ (see ESI,†) were treated as a function of proton concentration (according to eqn (9)), testing various kinetic models with a set of partial rate constants in order to obtain the best fit for the experimental data.

The dependence given in eqn (9) was used previously for description of kinetics of formation of Cu^{2+}–H_4L complex.[33] The set of experimental data for copper(II) complexation was extended to the pH region 5.0–7.0 compared with the original paper and re-fitted by eqn (9) with the same results as those reported in the original work.[33] The values of the particular rate constants are listed in Table 7 and the fit is included in Fig. 5. The ligand shows a high kinetic selectivity for complexation of Cu^{2+} ion in

Table 7 Summary of partial rate constants of formation of divalent metal ions complexes with H_4L (25 °C, 0.1 M KCl)

Rate constant/dm³ mol⁻¹ s⁻¹	Cu^{2+} [a]	Zn^{2+}	Cd^{2+}
$^{r}k_{H_4L}$	0.17(5)	—	0.15(5)
$^{r}k_{H_3L}$	1.4(2) × 10^3	7.4(1)	9.1(4)
$^{r}k_{H_2L}$	2.0(4) × 10^5	3.3(3) × 10^{2} [b]	1.3(2) × 10^2
$^{r}k_{OH}$	—	1.0 × 10^{5} [c]	—
$^{r}k_{H_3L}/^{r}k_{H_4L}$	8.2(3) × 10^3	46 [d]	61(20)
$^{r}k_{H_2L}/^{r}k_{H_3L}$	1.4(3) × 10^2	44(4)	14(2)

[a] Taken from ref. 33 (25 °C, 0.1 M (K,H)Cl). [b] Value of $^{r}k_{H_2L}$ = 1.0 dm³ mol⁻¹ s⁻¹ was reported for formation of Zn^{2+}-cyclam complex, ref. 65. [c] Rough estimate. Value of $^{r}k_{OH}/^{r}k_{H_2L}$ ratio is ~300. [d] Estimated values using an average value of $^{r}k_{H_4L}$ for Cu^{2+} and Cd^{2+} ions.

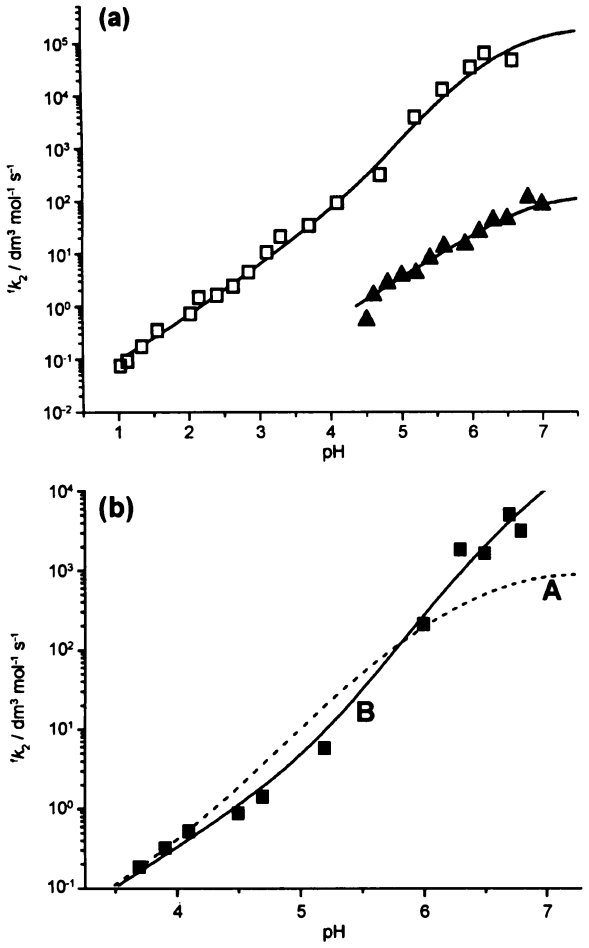

Fig. 5 The pH dependence of the second-order rate constant $^{r}k_2$ for the formation of complexes of 1,8-H_4te2p with divalent metal ions. (a) Fitting by eqn (9) (full lines) for Cu^{2+} (open squares) and Cd^{2+} (full triangles). (b) Fitting by eqn (10) (Zn^{2+}, full squares); line A (dashed) represents fitting by model with participation of H_3L^- and H_2L^{2-} species only; line B (full) represents the final model with rate constants corresponding to H_3L^- and H_2L^{2-} as well as $[Zn(OH)]^+$ (or HL^{3-}) species optimized simultaneously.

acid solutions (pH = 3.7–5.5, Fig. 5) over the other metal ions, and these experimental conditions have been already employed in analytical applications.[34,35] Both other metal ions (Zn^{2+}, Cd^{2+}) show a very similar reactivity in the pH region 3.7–5.5, but the formation of zinc(II) complexes is noticeably accelerated at higher

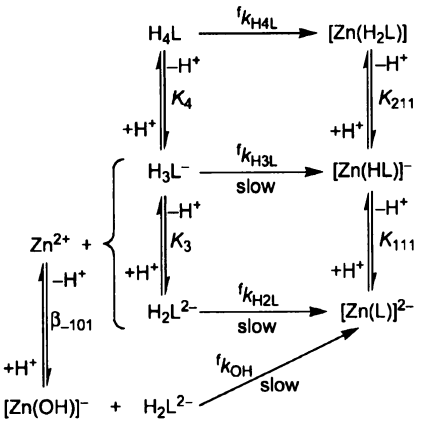

Scheme 4 Formation of zinc(II) complex of 1,8-H_4te2p.

pH (Fig. 5), where the kinetic selectivity of copper(II) complexation with respect to that of Zn^{2+} ion disappears.

In the case of Cd^{2+} ion, the experimental data can be sufficiently fitted by eqn (9) affording the values of rate constants for all three expected pathways, similarly as it was observed for copper(II) complexation (Table 7). In the case of zinc(II) complexation, the fit according to eqn (9) is in a good agreement with the experimental data at pH < 5; however, the acceleration at pH > 5.5 cannot be successfully described by eqn (9). Therefore, an additional reaction pathway must be taken into account. The acceleration can be attributed to the reaction of monohydroxo species $[Zn(OH)]^+$ (more correctly $[Zn(H_2O)_5(OH)]^+$ species) as, in general, hydroxo species are more reactive than aqua ions. The calculated speciation of metal hydroxo complexes in dependence on pH also supports this hypothesis, as $[Zn(OH)]^+$ is abundant in the pH range 5–6.8 (0.01–0.8%) (Fig. S11, ESI†). Furthermore, in the case of the other two metal ions, analogous hydroxo complexes are formed in appreciable abundance at much higher pH (Fig. S11, ESI†) and, therefore, their concentration in the pH range used for the complexations is negligible. Therefore, the reactions compiled in Scheme 4 were taken into account for zinc(II) complexation. According to Scheme 4, the dependence of the evaluated second-order rate constant on proton concentration can be derived similarly as in the previous case and is given by eqn (10) where $\alpha_{Zn} = 1 + \beta_{-101}/[H^+]$.

$$^{r}k_2 = \frac{^{r}k_{H_4L}\beta_4[H^+]^4 + {}^{r}k_{H_3L}\beta_3[H^+]^3 + {}^{r}k_{H_2L}\beta_2[H^+]^2 + {}^{r}k_{OH}\beta_2\beta_{-101}[H^+]}{\alpha_L\alpha_{Zn}} \quad (10)$$

However, for the zinc(II) system, the value of $^{r}k_{H_4L}$ could not be calculated due to numerical difficulties in fitting (the parameter was negative) but it is assumed to be of the same order of magnitude as for copper(II) and cadmium(II). This parameter is not important for the fitting and, therefore, it was not included in the further calculations, but the values of all other rate-constants can be determined from simultaneous fitting and are given in Table 7. The best fit is shown in Fig. 5. On the other hand, the same effect can be ascribed to the acceleration caused by the reaction of the monoprotonated ligand species, which gives the same pH-dependence of the rate constants due to the proton ambiguity. Analogous proton ambiguity and acceleration of complex formation was observed in a study of formation kinetics

of lead(II) with *N*,*N*′,*N*″,*N*‴-tetrakis(carbamoylmethyl)cyclam derivatives.[63] In our case, we suggest that involvement of the hydroxo species is correct as the effect was observed only for zinc(II) complexation, where the abundance (Fig. S11, ESI†) of hydroxo species is the highest among the studied metal ions. The H_2L^{2-} species exhibit a very compact solution structure stabilized by intramolecular hydrogen bonds and the structure is similar to that observed for H_4L in the solid state (Fig. S12, ESI†).[22] The final two dissociation constants of 1,8-H_4te2p are very high (much higher than those for cyclam or H_4teta), which leads to an extremely low concentration of monoprotonated species in the pH range employed.[22] In addition, the HL^{3-} species should have a low abundance even under equilibrium conditions as only one dissociation constant corresponding to last two dissociation steps could be determined.[22] Thus, we believe that pathway involving HL^{3-} species can be omitted. An acceleration of bound-to-bulk water exchange rates for monohydroxo-aqua complexes in comparison with aqua complexes was observed.[64] A relative acceleration of the pathway involving the $[Zn(OH)]^+$ and H_2L^{2-} species conforms to the range of accelerations of solvent exchange observed for the simple hydroxo-aqua species.

Monoprotonated ligand species were used for interpretation of an increased reactivity of several macrocyclic ligands in reactions of Zn^{2+} ion, such as cyclen ($^{f}k_{HL}$ = 1.3 × 10^5 dm^3 mol^{-1} s^{-1}),[65] cyclam ($^{f}k_{HL}$ = 7.5 × 10^4 and 5.0 × 10^4 dm^3 mol^{-1} s^{-1})[65,66] or H_4dota and H_4teta ($^{f}k_{HL}$ = 1.1 × 10^7 and 1.6 × 10^8 dm^3 mol^{-1} s^{-1}, respectively).[41] The data for these ligands were determined in a lower-pH region and the mechanism involving hydroxo species was not considered. To compare the rate constants for these ligands, we fitted our experimental data taking into account a rate constant corresponding to the HL^{3-} species instead of $^{f}k_{OH}$. The value of such rate constant (2.5 × 10^{10} dm^3 mol^{-1} s^{-1}) is higher than those above.

The highest rate found for the phosphonate ligand is in agreement with a generally accepted model for formation of complexes of polyazamacrocyclic ligands bearing ligating pendant arms.[67–69] In the mechanism, (partially) deprotonated pendant groups are rapidly bound to the metal aqua ion forming an intermediate complex.[42b,61] It is followed by a rate-determining step involving metal ion transfer into the macrocyclic cavity with simultaneous proton(s) removal from the protonated ring nitrogen atom(s) and/or ring conformation rearrangement. Phosphonate moiety exhibits the highest complex-forming ability (combination of its highest basicity and higher overall charge) among the ligands above (no pendant arms for cyclen and cyclam or carboxylate arms for H_4dota and H_4teta). Thus, it forms the most stable intermediate complex, mainly with hard metal ions. In addition, a high hydrogen bond-forming ability of phosphonate groups assists the removal of proton(s) from the macrocyclic cavity.

The formation reactions (characterized by the partial formation constants) for all three metal ions are much slower than water exchange for the corresponding aqua complexes. The highest rate observed for Cu^{2+} ion compared to the other ions reflects a generally fast ligand exchange observed for the ion due to Jahn–Teller effect and the fastest water exchange rate.[64] As relative differences in the formation rates between the ions are higher than differences in water exchange rate of the aqua ions, a high affinity of Cu^{2+} ion to nitrogen atoms of the ligand should be taken into account.[44b,61] This ion is probably the most easily transferred into the macrocyclic cavity in a rate-determining step. Despite a slower water exchange rate on zinc(II) aqua ion compared with cadmium(II) aqua ion, the title ligand reacts more quickly with Zn^{2+} than Cd^{2+} ion. If we accept a mechanism assumed for complexation of macrocycles with ligating side chains given above, the difference can be a consequence of a higher stability of a kinetic intermediate (where only phosphonate group(s) are bound) with small and hard Zn^{2+} ion.

To compare the reactivity of variously protonated species of 1,8-H_4te2p, the ratios of the partial rate constants were calculated (Table 7). In all cases, high values of the $^{f}k_{H_3L}/^{f}k_{H_4L}$ and $^{f}k_{H_2L}/^{f}k_{H_3L}$ ratios represent the complexation reaction acceleration. It can be caused by differences in charges of the species and/or easier structural rearrangement of less protonated ligand forms.[22] The highest differences in the $^{f}k_{H_3L}/^{f}k_{H_4L}$ and $^{f}k_{H_2L}/^{f}k_{H_3L}$ ratios for Cu^{2+} ion are similar to those reported for reactivity of various protonated forms of other cyclam derivatives with the ion.[70]

Dissociation kinetics of zinc(II) and cadmium(II) complexes

The dissociation kinetics of zinc(II) and cadmium(II) complexes of 1,8-H_4te2p was studied in the pH ranges 3.7–4.8 (Zn^{2+}) and 4.5–6.1 (Cd^{2+}), where the reactions occur with an optimal rate to be followed by conventional techniques. The dissociation of the zinc(II) complex was followed by UV-VIS spectroscopy using scavengers of either released ligand (Cu^{2+}) or Zn^{2+} (PAR) and the results of both methods are in a satisfactory agreement. This was verified from statistical point of view by analysis of experimental data from pH region 4.12–4.71 where the experimental points show the highest difference. The dissociation of the cadmium(II) complex was determined by the ligand scavenging with Cu^{2+} ion. The dependences of the pseudo-first-order rate dissociation constants on pH are given in Fig. 6 and the $^{d}k_{obs}$ are given in ESI.†

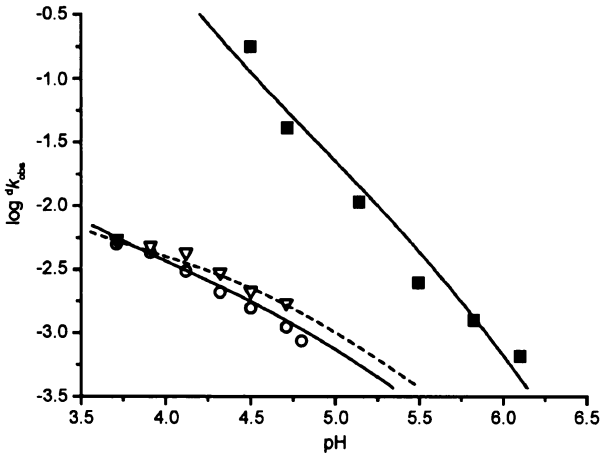

Fig. 6 The pH dependence of pseudo-first-order rate constants for dissociation of $[M(L)]^{2-}$ complexes; M = Zn^{2+} with Cu^{2+} (open circles, full line) and PAR (open triangles, dashed line) as scavengers, M = Cd^{2+} with Cu^{2+} as scavenger (full squares, full line). The experimental points were fitted by eqn (16) only (Zn^{2+}) or with the additional term corresponding to $[Cd(H_4L)]^{2+}$ species (Cd^{2+}) with the parameters listed in Table 8.

For fitting of the experimental data, the following mechanism can be suggested (Scheme 5). Here, the constants K_1–K_3

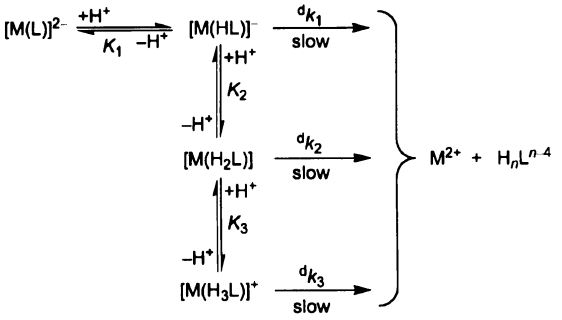

Scheme 5 The proposed reaction scheme for dissociation of $[M(L)]^{2-}$ complexes (M = Zn^{2+}, Cd^{2+}).

correspond to the protonation equilibrium of the complexes given by eqns (11)–(13) (charges are omitted).

$$K_1 = [M(HL)]/[M(L)][H] \quad (11)$$

$$K_2 = [M(H_2L)]/[M(HL)][H] \quad (12)$$

$$K_3 = [M(H_3L)]/[M(H_2L)][H] \quad (13)$$

The rate law for the proposed reaction mechanism is defined in eqn (14).

$$v = {}^{d}k_{obs}[complex]_{tot} = {}^{d}k_1[M(HL)] + {}^{d}k_2[M(H_2L)] + {}^{d}k_3[M(H_3L)] \quad (14)$$

In the given pH regions (3.7–4.8 for zinc(II) complex and 4.5–6.1 for cadmium(II) complex), only $[M(HL)]^-$ and $[M(H_2L)]$ species are present in a high abundance. The amounts of deprotonated complexes is negligible (Fig. 1) and the concentration of the $[M(H_3L)]^+$ complex should be also very low as value of $\log K_3$ for the $[M(H_3L)]^+$ species (Scheme 5) is much lower than that of $\log K_2$ for the $[M(H_2L)]$ species (*cf.* $\log K_3$ = 1.21 and 1.52 *vs.* $\log K_2$ = 5.15 and 5.27 reported for two isomeric $[Cu(H_3L)]^+$ and $[Cu(H_2L)]$ complexes;[33] $\log K_3$ = 1.15 and $\log K_2$ = 4.78 for *cis*-O,O-$[Ni(H_3L)]^+$ and *cis*-O,O-$[Ni(H_2L)]$ complexes[31]). Therefore, eqn (15) can be postulated.

$$v = {}^{d}k_{obs}[complex]_{tot} = {}^{d}k_{obs}([M(HL)] + [M(H_2L)]) \quad (15)$$

By rearrangement of eqns (11)–(15), the final rate law can be obtained (eqn (16)).

$${}^{d}k_{obs} = \frac{k_1 + {}^{d}k_2K_2[H^+] + {}^{d}k_3K_2K_3[H^+]^2}{1 + K_2[H^+]} \quad (16)$$

Eqn (16) formally corresponds to the equation used for fitting of acid-assisted dissociation data for the *pc*-$[Cu(H_4L)]^{2+}$ complex.[33] An analogous rate law has been described recently for dissociation of the lead(II) complex of *N*,*N*′,*N*″,*N*‴-tetrakis(carbamoylmethyl)cyclam.[63]

The pseudo-first-order rate constants, ${}^{d}k_{obs}$, for both divalent metal complexes were fitted through the experimental points by the eqn (16). The values of protonation constants, $\log K_2$ = 4.44 for zinc(II) and $\log K_2$ = 5.59, for cadmium(II) complexes, respectively, were taken from Table 2. The best fits of experimental data are shown in Fig. 6 and the resulting values in Table 8.

The dissociation pathways with participation of the $[M(HL)]^-$ complex species were not observed (${}^{d}k_1 = 0$). In the case of the zinc(II) complex, two reaction pathways of complex dissociation with two respective rate constants (for the $[Zn(H_2L)]$ and $[Zn(H_3L)]^+$ species) were resolved (Scheme 5). On the contrary, in the case of the cadmium(II) complex, the reaction pathways through triprotonated and, possibly, tetraprotonated species were identified, probably due to a very slow dissociation of the diprotonated species as only the upper limit of the corresponding rate constant ${}^{d}k_2$ could be estimated (Table 8). Involving a term corresponding to dissociation of the $[Cd(H_4L)]^{2+}$ species (${}^{d}k_4K_4K_3K_2[H^+]^3$) into eqn (16) led to a slight improvement of the fitting in the most acid region; the inclusion of this term did not change values in Table 8. However, only very rough estimate ${}^{d}k_4K_4K_3 \approx 5 \times 10^7$ $(dm^3\ mol^{-1})^2\ s^{-1}$ could be obtained for the $[Cd(H_4L)]^{2+}$ pathway. Comparing the dissociation rate constants of both metal complexes, decomposition reaction pathways involving the triprotonated species are much more important than other reaction steps involving the less ($[M(H_2L)]$) or, possibly, more protonated ($[Cd(H_4L)]^{2+}$) species under experimental conditions used in the study. This phenomenon can be demonstrated by the calculated ratio of the rate constants $({}^{d}k_3K_3)/{}^{d}k_2$ for both pathways for the zinc(II) complex (1.9×10^3) while this ratio is even higher by several orders of magnitude for the cadmium(II) complex. It can be assumed that both $[M(H_2L]$ species are hardly protonated and corresponding protonation constant of the $[M(H_2L)]$ species should be in range of $\log K_3$ = 1–2. Therefore, the concentration of the triprotonated reaction intermediates is on a trace level under the experimental conditions used in this study. Their high reactivity is probably caused by the fact that the third proton can be very easily transferred to a nitrogen atom leading to fast decomposition of such complex species. The overall inertness of the complexes decreases in the order Cu(II) ≫ Zn(II) > Cd(II). This trend is related to the metal ion size (fitting the macrocyclic cavity) and

Table 8 Summary of partial dissociation rate constants determined (eqn 16) for acid-assisted hydrolysis of $[M(L)]^{2-}$ complexes (M = Zn^{2+}, Cd^{2+}) (25 °C, 0.1 M KCl)

		Zn^{2+}		
Rate constant	Cu^{2+} [a]	PAR scavenger	Cu^{2+} scavenger	Cd^{2+}
${}^{d}k_2/s^{-1}$	$8.5(3) \times 10^{-4}$	$4.6(5) \times 10^{-3}$	$3.2(1) \times 10^{-3}$	$<3 \times 10^{-4}$ [b]
${}^{d}k_3K_3/dm^3\ mol^{-1}\ s^{-1}$	$9.7(1.2) \times 10^{-5}$	8.9(1.3)	17.6(1.2)	$2.48(6) \times 10^3$
$({}^{d}k_3K_3/{}^{d}k_2)/dm^3\ mol^{-1}$	0.114(6)	$1.9(3) \times 10^3$	$5.5(4) \times 10^3$	$>10^7$

[a] Reported[33] for *pc*-$[Cu(H_4L)]^{2+}$ complex species, t = 25.0 °C, I = 5.0 M $(Na,H)ClO_4$. [b] Only an upper estimate.

their affinity to nitrogen or oxygen atoms (strength of the M^{2+}–N and M^{2+}–O bonds).

Conclusions

We have studied interactions of divalent metal ions with a bis(methylphosphonate) cyclam derivative. In the solid state, the structures of the complexes clearly depend on the relative affinity of the central ion to different donor atoms of the ligand. The diprotonated zinc(II) complex is mononuclear with all available donor atoms coordinated. In both diprotonated manganese(II) and lead(II) complexes, the central metal ion binds only oxygen donors and nitrogen atoms are unbound and protonated. The determination of stability constants reveals a high preference of complexation of transition-metal ions, and in particular a high selectivity to the Cu^{2+} ion. In the complexes with transition metals, the nitrogen atoms of the macrocycle are coordinated to the metal ion from the beginning of the complexation in acid solutions. The ligand has a low affinity to alkaline earth ions, and the nitrogen atoms are coordinated to the central metal ions only in strongly alkaline solutions, similarly as it was found for other cyclam derivatives. The behaviour of lead(II) and manganese(II) complexes is somewhere in between the previous groups, with deprotonation of the amino groups induced by metal in slightly alkaline region. The kinetics of formation of zinc(II) and cadmium(II) complexes follows the common mechanism assumed for complex formation of macrocycles bearing coordinating pendant arms. It shows a high difference in reactivity between differently protonated ligand species. Complexes of Zn^{2+} and Cd^{2+} ions are rather unstable in acid-assisted decomplexation in comparison with the corresponding copper(II) and nickel(II) complexes. The zinc(II) complex is much more kinetically inert than the cadmium(II) complex (Fig. 6). This inertness is associated with the suitability of the size and conformation of the macrocycle cavity. The smaller metal ions such as Cu^{2+} or Zn^{2+} fit the cavity better than the larger ones as Cd^{2+} ion. The results confirm that 1,8-H_4te2p is a very suitable ligand for selective binding of divalent copper, *e.g.* in nuclear medicine applications.

Acknowledgements

We thank Dr K. Lang (Institute of Inorganic Chemistry, Academy of Sciences of the Czech Republic) for the use of stopped-flow apparatus and Dr I. Císařová for X-ray data acquisition. This work was supported by the Grant Agency of the Czech Republic (No. 203/06/0467) and EU FP6 Network of Excellence EMIL (No. LSHC-2004-503569) and DiMI (No. LSHB-2005-512146) projects.

References

1 A. E. Martell and R. D. Hancock, *Metal Complexes in Aqueous Solutions*, Plenum Press, New York, 1996.
2 S. F. Lincoln, *Coord. Chem. Rev.*, 1997, **166**, 255.
3 K. P. Wainwright, *Coord. Chem. Rev.*, 1997, **166**, 35.
4 M. Meyer, V. Dahaoui-Ginderey, C. Lecomte and R. Guilard, *Coord. Chem. Rev.*, 1998, **178–180**, 1313.
5 L. F. Lindoy, *Adv. Inorg. Chem.*, 1998, **45**, 75.
6 S. Aime, M. Botta, M. Fasano and E. Terreno, *Acc. Chem. Res.*, 1999, **32**, 941.
7 P. Caravan, J. J. Ellison, T. J. Mc Murry and R. B. Laufer, *Chem. Rev.*, 1999, **99**, 2293.
8 A. E. Merbach and É. Tóth, *The Chemistry of Contrast Agents in Medical Magnetic Resonance Imaging*, Wiley, Chichester, UK, 2001.
9 *Topics in Current Chemistry*, Springer, Heidelberg, Germany, 2002, vol. 221.
10 C. J. Anderson and M. J. Welch, *Chem. Rev.*, 1999, **99**, 2219.
11 W. A. Volkert and T. J. Hoffmann, *Chem. Rev.*, 1999, **99**, 2269.
12 (*a*) S. Liu, *Chem. Soc. Rev.*, 2004, **33**, 445; (*b*) S. Liu and D. S. Edwards, *Bioconjugate Chem.*, 2001, **12**, 7.
13 *Handbook of Radiopharmaceuticals. Radiochemistry and Applications*, ed. M. J. Welch and C. S. Redvanly, Wiley, Chichester, UK, 2003.
14 W. P. Li, L. A. Meyer and C. J. Anderson, *Top. Curr. Chem.*, 2005, **252**, 179.
15 D. Parker, R. S. Dickins, H. Puschmann, C. Crossland and J. A. K. Howard, *Chem. Rev.*, 2002, **102**, 1977.
16 S. Faulkner and J. L. Matthews, in *Comprehensive Coordination Chemistry II*, ed. J. A. McCleverty and T. J. Meyer, Elsevier, 2004, vol. 9, pp. 913–944.
17 S. V. Smith, *J. Inorg. Biochem.*, 2004, **98**, 1874.
18 S. Hassfjell and M. W. Brechbiel, *Chem. Rev.*, 2001, **101**, 2019.
19 I. Belskii, Y. M. Polikarpov and M. I. Kabachnik, *Usp. Khim.*, 1992, **61**, 415, and references therein.
20 A. D. Sherry, *J. Alloys Compd.*, 1997, **249**, 153.
21 I. Lukeš, J. Kotek, P. Vojtíšek and P. Hermann, *Coord. Chem. Rev.*, 2001, **216–217**, 287, and references therein.
22 J. Kotek, P. Vojtíšek, I. Císařová, P. Hermann, P. Jurečka, J. Rohovec and I. Lukeš, *Collect. Czech. Chem. Commun.*, 2000, **65**, 1289.
23 A. D. Sherry, J. Ren, J. Huskens, E. Brücher, E. Tóth, C. F. C. G. Geraldes, M. M. C. A. Castro and W. P. Cacheris, *Inorg. Chem.*, 1996, **35**, 4604.
24 X. Sun, M. Wuest, Z. Kovacs, A. D. Sherry, R. Motekaitis, Z. Wang, A. E. Martell, M. J. Welch and C. J. Anderson, *J. Biol. Inorg. Chem.*, 2003, **8**, 217.
25 (*a*) K. Popov, H. Ronkkomaki and L. H. J. Lajunen, *Pure Appl. Chem.*, 2001, **73**, 1641; (*b*) K. Popov, E. Niskanen, H. Rönkkömäki and L. H. J. Lajunen, *New J. Chem.*, 1999, **23**, 1209.
26 (*a*) F. Marques, L. Gano, M. P. Campello, S. Lacerda, I. Santos, L. M. P. Lima, J. Costa, P. Antunes and R. Delgado, *J. Inorg. Biochem.*, 2006, **100**, 270; (*b*) K. P. Guerra, R. Delgado, L. M. P. Lima, M. G. B. Drew and V. Félix, *Dalton Trans.*, 2004, 1812; (*c*) F. Marques, K. P. Guerra, L. Gano, J. Costa, M. P. Campello, L. M. P. Lima, R. Delgado and I. Santos, *J. Biol. Inorg. Chem.*, 2004, **9**, 859; (*d*) R. Delgado, L. C. Siegfried and T. A. Kaden, *Helv. Chim. Acta*, 1990, **73**, 140.
27 I. Lázár, A. D. Sherry, R. Ramasamy, E. Brücher and R. Király, *Inorg. Chem.*, 1991, **30**, 5016.
28 K. Bazakas and I. Lukeš, *J. Chem. Soc., Dalton Trans.*, 1995, 1133.
29 (*a*) P. Lubal, M. Kývala, P. Hermann, J. Holubová, J. Rohovec, J. Havel and I. Lukeš, *Polyhedron*, 2001, **20**, 47; (*b*) J. Rohovec, M. Kývala, P. Vojtíšek, P. Hermann and I. Lukeš, *Eur. J. Inorg. Chem.*, 2000, 195.
30 M. Helps, D. Parker, J. R. Murphy and J. Chapman, *Tetrahedron Lett.*, 1989, **45**, 219.
31 J. Kotek, P. Vojtíšek, I. Císařová, P. Herman and I. Lukeš, *Collect. Czech. Chem. Commun.*, 2001, **66**, 363.
32 J. Kotek, I. Císařová, P. Hermann, I. Lukeš and J. Rohovec, *Inorg. Chim. Acta*, 2001, **317**, 324.
33 J. Kotek, P. Lubal, P. Hermann, I. Císařová, I. Lukeš, T. Godula, I. Svobodová, P. Táborský and J. Havel, *Chem. Eur. J.*, 2003, **9**, 233.
34 I. Svobodová, P. Lubal, P. Hermann, J. Kotek and J. Havel, *J. Inclusion Phenom. Macrocycl. Chem.*, 2004, **49**, 11.
35 I. Svobodová, P. Lubal, P. Hermann, J. Kotek and J. Havel, *Microchim. Acta*, 2004, **148**, 21.
36 (*a*) R. Přibil, *Analytical Applications of EDTA and Related Compounds*, Pergamon Press, Oxford, 1972; (*b*) G. Schwarzenbach and H. Flaschka, *Complexometric Titrations*, Methuen, London, 1969.
37 (*a*) M. Kývala and I. Lukeš, *Chemometrics'95*, Abstract book p. 63, Pardubice, Czech Republic, 1995; full version of *OPIUM software package* is available (free of charge) on http://www.natur.cuni.cz/~kyvala/opium.html; (*b*) M. Kývala, P. Lubal and I. Lukeš, *IX. Spanish–Italian, and Mediterranean Congress on Thermodynamics of Metal Complexes (SIMEC 98)*, Girona, Spain, 1998.
38 (*a*) A. E. Martell and R. M. Smith, *Critical Stability Constants*, Plenum Press, New York, 1974–1989, vol. 1–6; (*b*) *NIST Standard*

Reference Database 46 (Critically Selected Stability Constants of Metal Complexes), Version 7.0, 2003.
39 C. F. Baes, Jr. and R. E. Mesmer, *The Hydrolysis of Cations*, Wiley, New York, 1976.
40 Y. Zhang and M. Muhammed, *Hydrometallurgy*, 2001, **60**, 215.
41 S. P. Kasprzyk and R. G. Wilkins, *Inorg. Chem.*, 1982, **21**, 3349.
42 (*a*) E. Balogh, R. Tripier, R. Ruloff and É. Tóth, *Dalton Trans.*, 2005, 1058; (*b*) K.-Y. Choi, D. W. Kim, C. S. Kim, C. P. Hong, H. Ryu and Y.-I. Lee, *Talanta*, 1997, **44**, 527; (*c*) É. Tóth, E. Brücher, I. Lázár and I. Tóth, *Inorg. Chem.*, 1994, **33**, 4070; (*d*) K.-Y. Choi, J. C. Kim and D. W. Kim, *J. Coord. Chem.*, 1993, **30**, 1.
43 E. J. Billo, *Excel for Chemists*, Wiley-VCH, New York, 2001.
44 Z. Otwinowski and W. Minor, *HKL Denzo and Scalepack Program Package by Nonius BV*, Delft, 1997; Z. Otwinowski and W. Minor, *Methods Enzymol.*, 1997, **276**, 307.
45 A. Altomare, M. C. Burla, M. Camalli, G. L. Cascarano, C. Giacovazzo, A. Guagliardi, A. G. G. Moliterni, G. Polidori and R. Spagna, *J. Appl. Crystallogr.*, 1999, **32**, 115.
46 G. M. Sheldrick, *SHELXL97. Program for Crystal Structure Refinement from Diffraction Data*, University of Gottingen, Gottingen, 1997.
47 X. Liang and P. J. Sadler, *Chem. Soc. Rev.*, 2004, **33**, 246.
48 M. K. Moi, C. F. Meares, M. J. McCall, W. C. Cole and S. J. DeNardo, *Anal. Biochem.*, 1985, **148**, 249.
49 S. Füzerová, J. Kotek, I. Císařová, P. Hermann, K. Binnemans and I. Lukeš, *Dalton Trans.*, 2005, 2908.
50 S. A. Pisareva, F. I. Belskii, T. Ya. Medved and M. I. Kabachnik, *Izv. Akad. Nauk SSSR, Ser. Khim.*, 1987, 413.
51 G. Anderegg, F. Arnaud-Neu, R. Delgado, J. Felcman and K. Popov, *Pure Appl. Chem.*, 2005, **77**, 1445.
52 (*a*) S. Chaves, R. Delgado and J. J. R. Frausto Da Silva, *Talanta*, 1992, **39**, 249; (*b*) R. Delgado and J. J. R. Frausto Da Silva, *Talanta*, 1982, **29**, 815.
53 (*a*) F. Marques, L. Gano, M. P. Campello, S. Lacerda, I. Santos, L. M. P. Lima, J. Costa, P. Antunes and R. Delgado, *J. Inorg. Biochem.*, 2006, **100**, 270; (*b*) R. Delgado, J. Costa, K. P. Guerra and L. M. P. Lima, *Pure Appl. Chem.*, 2005, **77**, 569.
54 X. Liang, M. Weishäupl, J. A. Parkinson, S. Parsons, P. A. McGregor and P. J. Sadler, *Chem. Eur. J.*, 2003, **9**, 4709.
55 B. Bosnich, C. K. Poon and M. Tobe, *Inorg. Chem.*, 1965, **4**, 1102.
56 A. Riesen, M. Zehnder and T. A. Kaden, *Acta Crystallogr., Sect. C*, 1991, **47**, 531.
57 (*a*) B.-P. Yang, Z.-M. Sun and J.-G. Mao, *Inorg. Chim. Acta*, 2004, **357**, 1583; (*b*) J.-L. Song, J.-G. Mao, Y.-Q. Sun, H.-Y. Zeng, R. K. Kremer and A. Clearfield, *J. Solid State Chem.*, 2004, **177**, 633; (*c*) C. Lei, J.-G. Mao and Y.-Q. Sun, *J. Solid State Chem.*, 2004, **177**, 2449; (*d*) Z.-M. Sun, J.-G. Mao, B.-P. Yang and S.-M. Ying, *Solid State Sci.*, 2004, **6**, 295; (*e*) J.-G. Mao, Z. Wang and A. Clearfield, *J. Chem. Soc., Dalton Trans.*, 2002, 4541.
58 S.-M. Ying, J.-G. Mao, B. P. Yang and Z.-M. Sun, *Inorg. Chem. Commun.*, 2003, **6**, 1319.
59 (*a*) F. H. Allen, *Acta Crystallogr., Sect. B*, 2002, **58**, 380; (*b*) A. G. Orpen, *Acta Crystallogr., Sect. B*, 2002, **58**, 398.
60 D. Kong, D. G. Medvedev and A. Clearfield, *Inorg. Chem.*, 2004, **43**, 7308.
61 K.-Y. Choi, *Polyhedron*, 1997, **16**, 2073.
62 R. G. Wilkins, *Kinetics and Mechanism of Reactions of Transition Metal Complexes*, VCH, Weinheim, 1991.
63 F. Cuenot, M. Meyer, E. Espinosa and R. Guilard, *Inorg. Chem.*, 2005, **44**, 7895.
64 D. T. Richens, *Chem. Rev.*, 2005, **105**, 1961.
65 M. Kodama and E. Kimura, *J. Chem. Soc., Dalton Trans.*, 1977, 2269.
66 P. Leugger, L. Hertli and T. A. Kaden, *Helv. Chim. Acta*, 1978, **61**, 2296.
67 E. Brücher, *Top. Curr. Chem.*, 2002, **221**, 123.
68 M. Soibinet, D. Gusmeroli, L. Siegfried, T. A. Kaden, C. Palivan and A. Schweiger, *Dalton Trans.*, 2005, 2138.
69 J. Moreau, E. Guillon, J.-C. Pierrard, J. Rimbault, M. Port and M. Aplincourt, *Chem. Eur. J.*, 2004, **10**, 5218.
70 P. G. Lye, G. A. Lawrance and M. Maeder, *J. Chem. Soc., Dalton Trans.*, 2001, 2376.

CREATED USING THE RSC ARTICLE TEMPLATE (VER. 3.0) - SEE WWW.RSC.ORG/ELECTRONICFILES FOR DETAILS

ARTICLE TYPE www.rsc.org/xxxxxx | XXXXXXXX

Coordination properties of cyclam (1,4,8,11-tetraazacyclotetradecane) endowed with two methylphosphonic acid pendant arms in the 1,4-positions†

Jana Havlíčková,[a] Hana Medová,[a] Tomáš Vitha,[a] Jan Kotek,[a,*] Ivana Císařová[a] and Petr Hermann[a]

Received (in XXX, XXX) 1st January 2007, Accepted 1st January 2007
First published on the web 1st January 2007
DOI: 10.1039/b000000x

The title ligand, 1,4,8,11-tetraazacyclotetradecane-1,4-diyl-bis(methylphosphonic acid) (H_4te2p^{1,4}, H_4L), was prepared by an optimized synthetic approach and its complexing properties towards selected metal ions were studied by means of potentiometry. The ligand forms very stable complex with copper(II) (logβ(CuL) = 27.21), with a high selectivity over binding of other metal ions (*i.e.* logβ(ZnL) = 20.16, logβ(NiL) = 21.92). The crystal structures of two intermediates in the ligand synthesis and two forms of the nickel(II) complex (obtained by crystallization at various pH) were determined. From acid solution, the crystals of *trans*-O,O-[Ni(H_3L)]Cl·H_2O were isolated. In such complex species, one phosphonate pendant arm is double- and the second arm is monoprotonated. The isolation of such species demonstrates a high kinetic inertness of the complex. The central metal ion is surrounded by four *in plane* nitrogen atoms (in the ring configuration **III**) and two oxygen atoms of pendant moieties in the apical positions of octahedral sphere. From neutral solution, the crystals of {*trans*-O,O-[Ni(H_2L)]}$_3$·5H_2O were isolated. The molecular structures of the complex units found in this structure are analogous to the previous one.

Introduction

Most of studies on macrocyclic ligands have been focused on derivatives bearing additional coordinating pendant groups which influence both thermodynamic stability and kinetics of the complexation/decomplexation. Among the macrocycles, 1,4,8,11-tetraazacyclotetradecane (cyclam, Chart 1) is one of the most studied azacycles.[1,2] Cyclams (fourteen-membered tetraamine macrocycles) show ability to complex first-row transition metal cations, especially copper(II), and the complexes are often highly thermodynamically stable and kinetically inert.[3]

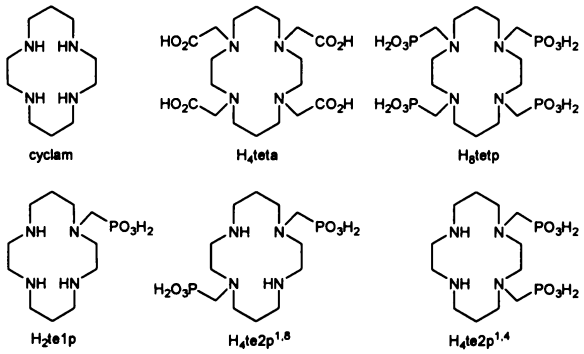

Chart 1 Structures of ligands mentioned in the text.

The investigations of the cyclam-derived ligands and their complexes is often motivated by their use in medicine.[3,4] It was found that cyclam-based anti-HIV agents are even more active *in vivo* in the form of complexes with several metal ions.[3,5] The macrocyclic ligands are used as chelators of the metal radioisotopes in targeted radiopharmaceuticals.[3,6] For the utilizations in nuclear medicine, macrocyclic ligands are generally preferred to open-chain ligands due to higher stability and mainly higher inertness of their complexes. Among metal radioisotopes, the copper radionuclides (especially ^{64}Cu and ^{67}Cu) seem to be very perspective. They undergo various decays, exhibit promising properties for application in both scintigraphic imaging (single-photon imaging and positron emission tomography) as well as in targeted radiotherapy.[7] The ligands based on the cyclam skeleton offer an excellent binding environment for Cu(II) ion as the ion ideally fits the macrocyclic cavity.[3,8] Chelators utilized for complexation of copper radionuclides are often based on 1,4,8,11-tetraazacyclotetradecane-1,4,8,11-tetraacetic acid (H_4teta, Chart 1). However, such ligands have more donor atoms (8) than it is required by copper(II) ion (5–6) and, therefore, several pendant arms remain non-coordinated in the copper(II) complexes.[9] It was shown, that such copper(II) complexes are not optimal for biomedical applications as they lose the metal ion *in vivo*.[10]

The investigations of macrocycles derivatized with four methylphosphonic acid (–CH_2–PO_3H_2)[11] or methylphosphinic acid (–CH_2–P(R)O_2H)[12] pendant arms (Chart 1) have started several years ago. However, similarly to the H_4teta derivatives, the ligands have more coordinating atoms and the ligands should be rather considered as derivatives of *N,N',N'',N'''*-tetramethylcyclam which forms generally kinetically less inert complexes than cyclam itself.[13] Therefore, copper(II) complexes of cyclam derivatives having a smaller number of pendant arms has been studied. The studies involved ligands with one carboxylic acid[14] or pyridine[15] pendant arm, or two acetate,[16,17] amine,[17] acetamide[17,18] or pyridine[19,20] coordinating pendant arms.

We have already prepared cyclam substituted with only one pendant arm[21] or with two methylphosphonic acid pendant arms in "*trans*" (1,8-) positions (H_2te1p and H_4te2p[1,8], Chart 1).[22] Both ligands form extremely stable copper(II) complexes,[21,23] and the complexation reaction was found to be very selective for copper(II) over zinc(II).[24] We prepared the title ligand, 1,4,8,11-tetraazacyclotetradecan-1,4-diyl-bis(methylphosphonic acid) (H_4te2p[1,4], H_4L, Chart 1),[25] but a scaling up of synthesis based on the original procedure was complicated by extensive chromatographic separations. So, we decided to develop another synthesis, based on previously reported oxalyl-bis(amide) protection.[26] Here, we report on the optimized ligand synthesis and the investigations of complexing properties of H_4te2p[1,4] towards selected divalent metal ions.

Experimental

Chemicals

Cyclam[27] and compounds **1**–**3**[26] were synthesised by published methods. Paraformaldehyde was filtered from aged aqueous solutions of formaldehyde (Lachema) and was dried in desiccator over conc. H_2SO_4. All other chemicals were used as received from commercial sources. Metal ion stock solutions were prepared by dissolution of recrystallized $M(NO_3)_2{\cdot}xH_2O$ in deionized water; the metal content was determined by titration with Na_2H_2edta solution. A standard nitric acid solution was prepared by passing of an aqueous potassium nitrate solution through a Dowex 50W-8 (H^+-form) column. A carbonate-free KOH (~0.2 M) solution was standardized against potassium hydrogen phthalate and the HNO_3 (~0.03 M) solution against the KOH solution.

Instrumental Methods

NMR spectra were recorded on a Varian VNMRS300 spectrometer operating at 299.9 (^{1}H), 75.4 (^{13}C) and 121.4 (^{31}P) MHz. NMR spectra references: tetramethylsilane for $CDCl_3$ solutions (δ_H,δ_C = 0 ppm) and *t*-BuOH for D_2O solutions (δ_H = 1.25 ppm, δ_C = 32.0 ppm) as an internal and 85% D_3PO_4 in D_2O (δ_P = 0.0 ppm) as an external references. Chemical shifts δ are given in ppm and coupling constants J are reported in Hz. Abbreviations of signal multiplicities: s (singlet), d (doublet), t (triplet), q (quartet), p (pentet), m (multiplet) and br (broad). The ESI-MS spectra were acquired on a Bruker ESQUIRE 3000 spectrometer with ion-trap detection in both positive and negative modes. Thin layer chromatography (TLC) was performed on aluminium sheets Silica gel 60 F254 (Merck KGaA, Germany) using 2-propanol:conc. aq. NH_3:water 7:3:3 mixture as mobile phases with ninhydrin spray or dipping of the sheets in 5% aqueous solution of $CuSO_4$ detection. Elemental analyses were done in the Institute of Macromolecular Chemistry (Academy of Sciences of the Czech Republic, Prague).

Synthesis

Isolation of 1,5,8,12-tetraazabicyclo[10.2.2]hexadecane-13,14-dione, 1

Due to problematic isolation of **1** as a free base according to ref.[26], we isolated the compound as dihydrochloride salt as it follows. Reaction mixture from the original synthesis[26] (5 mmol scale, 1.00 g of cyclam) was evaporated to dryness, and re-dissolved in 15 ml of ethanol. Concentrated aq. HCl (1 ml) was added dropwise and the white precipitate was collected by filtration and dried in dessiccator (1.36 g, 83 %). (Found C, 43.9; H, 7.2; Cl, 22.0; N, 17.0. Calc. for **1**·2HCl, $C_{12}H_{24}Cl_2N_4O_2$, M = 327.3: C, 44.0; H, 7.4; Cl, 21.7; N, 17.1%). Colourless needles of **1**·2HCl suitable for X-ray diffraction were prepared by vapour diffusion of ethanol to aq. solution of **1**·2HCl, acidified by a drop of a diluted aq. HCl.

Isolation of 1,4-dibenzyl-1,4,8,11-tetraazacyclotetradecane, 3

After hydrolysis of **2** in aq. NaOH, extraction of **3** to chloroform and evaporation,[26] the compound was isolated by crystallization from concentrated aq. HBr (75 %, based on **1**·2HCl) as an off-white solid. (Found C, 37.7; H, 6.0; Br, 41.6; N, 7.2. Calc. for **3**·4HBr·4H_2O, $C_{24}H_{48}Br_4N_4O_4$, M = 776.3: C, 37.1; H, 6.2; Br, 41.2; N, 7.2%). Colourless plates of **3**·4HBr·2H_2O were formed by slow cooling of hot solution of **3** in diluted (1:1) aq. HBr.

Synthesis of 8,11-dibenzyl-1,4-bis(diethoxyphosphoryl methyl)-1,4,8,11-tetraazacyclotetradecane, 4

Compound **3**·4HBr·4H_2O (5.45 g, 7.0 mmol) was dissolved in water (100 ml) and NaOH (5 g) was added. Free base **3** was extracted by $CHCl_3$ (3×50 ml), extracts were combined and dried over Na_2SO_4. Mixture was filtered and the solvent was evaporated. The macrocycle was dissolved in triethyl phosphite (11.6 g, 74 mmol, 10 equiv.). Paraformaldehyde (1.10 g, 37 mmol, 5 equiv.) was added and the mixture was stirred at 75 °C for 4 d in a closed flask. Reaction mixture was poured onto column of strong cation exchanger (Dowex 50, 100 ml, H^+-form). The non-cyclic compounds were eluted by EtOH:water (3:1, 500 ml) mixture. The product **4** was collected by EtOH:conc. aq. NH_3 (5:1, 250 ml) mixture. After evaporation, the product was isolated as a brownish oil. TLC (ninhydrine) brown spot, R_f = 0.9; δ_H($CDCl_3$) 1.31 (12 H, m, CH_3), 1.62 (4 H, p, $^3J_{HH}$ 6.8, $CH_2CH_2CH_2$), 2.59 (4 H, t, $^3J_{HH}$ 6.8, $NCH_2CH_2CH_2N$), 2.62 (4 H, s, NCH_2CH_2N), 2.70 (4 H, t, $^3J_{HH}$ 6.8, $NCH_2CH_2CH_2N$), 2.79 (4 H, s, NCH_2CH_2N), 2.95 (4 H, d, $^2J_{PH}$ 10.0, CH_2P), 3.48 (4 H, s, CH_2Ph), 4.12 (8 H, m, OCH_2) and 7.2–7.6 (10 H, m, arom); δ_C($CDCl_3$) 17.0 (4 C, CH_3), 25.0 (2 C, $CH_2CH_2CH_2$), 51.0 (2 C, d, $^1J_{PC}$ 628, CH_2P), 51.2 (2 C, $PhCH_2NCH_2$), 52.4 (2 C, $PhCH_2NCH_2$), 53.2 (2 C, d, $^3J_{PC}$ 35.2, PCH_2NCH_2), 54.1 (2 C, d, $^3J_{PC}$ 35.2, PCH_2NCH_2), 60.3 (2 C, $PhCH_2$), 63.3 (4 C, d, $^2J_{PC}$ 148, OCH_2), 128.3 (2 C, arom), 129.3 (4 C, arom), 130.5 (4 C, arom), 140.0 (2 C, arom CCH_2); δ_P($CDCl_3$) 31.1 (br s).

Synthesis of 8,11-dibenzyl-1,4,8,11-tetraazacyclotetradecane-1,4-diyl-bis(methylphosphonic acid), 5

The matter obtained above was dissolved in diluted aq. HCl (1:1, 70 ml) and the mixture was heated under reflux for 24 h. The volatiles were evaporated and the residue was dissolved in a small amount of water and poured onto column of strong cation exchanger (Dowex 50, 100 ml, H^+-form). The column was washed by water till neutrality of the eluate and the product **5** was collected with 5% aq. HCl. Fractions containing the product were evaporated, re-dissolved in water and chromatographed on column of weak cation exchanger (Amberlite CG50, 50 ml, H^+-form) with 3% aq. HCl as a mobile phase. Fractions containing pure product (TLC check)

were combined, and the product was crystallized from hot water with few drops of conc. aq. HCl. The white hydrochloride salt was collected by filtration and dried in air (1.66 g, 33%, based on **3**·4HBr·4H_2O). (Found C, 43.3; H, 7.0; Cl, 15.2; N, 7.7; P, 8.6. Calc. for **5**·3HCl·2H_2O, $C_{26}H_{49}Cl_3N_4O_8P_2$, M = 714.0: C, 43.7; H, 6.9; Cl, 14.9; N, 7.8; P, 8.7%); TLC (ninhydrine) purple spot, R_f = 0.6; δ_H(D_2O/NaOD, pD = 13.8) 1.68 (4 H, br, $CH_2CH_2CH_2$), 2.53 (8 H, br+s, $CH_2CH_2CH_2$ + NCH_2CH_2N), 2.64 (4 H, d, $^2J_{PH}$ 10.7, CH_2P), 2.75 (4 H, br, $CH_2CH_2CH_2$), 2.86 (4 H, s, NCH_2CH_2N), 3.49 (4 H, s, CH_2Ph), 7.16 (4 H, m, arom) and 7.32 (6 H, m, arom); δ_C(D_2O/NaOD, pD = 13.8) 21.2 (2 C, *C*CC), 45.4 (2 C, *C*CC), 49.8 (2 C, CC*C*), 52.7 (2 C, N*C*CN), 53.2 (2 C, NC*C*N), 57.0 (2 C, d, $^1J_{CP}$ 142, *C*P), 61.4 (2 C, *C*Ph), 129.9 (2 C, arom), 130.8 (4 C, arom), 132.1 (4 C, arom), 139.4 (2 C, arom); δ_P(D_2O/NaOD, pD = 13.8) 16.7 (t, $^2J_{PH}$ 11.8); *m/z* (ESI) +569.4 ([M+H]$^+$, $C_{26}H_{43}N_4O_6P_2^+$ requires 569.3), –567.3 ([M–H]$^-$, $C_{26}H_{41}N_4O_6P_2^-$ requires 567.3).

Attempt of synthesis of 1,4-bis(diethoxyphosphorylmethyl)-1,4,8,11-tetraazacyclotetradecane, 6

Compound **4** (0.32 g) was dissolved in EtOH (10 ml) in double-necked flask (50 ml) under argon. To the solution, a 10% Pd/C catalyst (0.20 g) was added. The flask was flushed with hydrogen, and the mixture was stirred under hydrogen atmosphere for 12 h. New portion of catalyst (0.20 g) was added and the mixture was stirred for further 24 h. After that time, a sample of the mixture was filtered off, evaporated to dryness and analyzed by NMR. According to ^{1}H NMR, complete debenzylation occurred, but three major peaks appeared in the ^{31}P NMR spectrum at 29.5 (15 %), 31.3 (65 %) and 31.8 (20 %) ppm. Trial of deesterification of the product mixture in dry HBr/AcOH solution (30% w/w) led to a more complicated mixture (5 peaks in ^{31}P NMR spectrum at 11.1 (15 %), 11.6 (15 %), 11.9 (40 %), 12.9 (20 %) and 14.0 (10 %) ppm).

Synthesis of 1,4,8,11-tetraazacyclotetradecane-1,4-diyl-bis(methylphosphonic acid) , H_4te2p^{1,4} (H_4L)

Compound **5**·3HCl·2H_2O (1.40 g, 2.1 mmol) was dissolved in mixture of water (15 ml) and AcOH (10 ml) in double-necked flask (50 ml) under argon. To the solution, a 10% Pd/C catalyst (0.15 g) was added. The flask was flushed with hydrogen and the mixture was stirred under hydrogen atmosphere for 24 h. The catalyst was filtered off and the solution was evaporated to dryness. The residue was dissolved in a small amount of water and poured onto column of strong cation exchanger (Dowex 50, 100 ml, H^+-form). The column was washed by water till neutrality of the eluate and the product H_4te2p^{1,4} was collected by 5% aq. ammonia. Fractions containing the product were evaporated to dryness. The residue was re-dissolved in water and chromatographed on column of weak cation exchanger (Amberlite CG50, 50 ml, H^+-form) with water. The product was crystallized from conc. aqueous solution by a slow addition of acetone. The white solid H_4te2p^{1,4}·4H_2O was collected by filtration and dried in air (0.52 g, 54 %). The characteristics were identical to those reported.[25]

Preparation of *trans*-O,O-[Ni(H_3L)]Cl·H_2O

Ligand (50 mg of H_4te2p^{1,4}·4H_2O, 0.11 mmol) was dissolved with equimolar amount of $NiCl_2$·6H_2O (26 mg) in water (2 ml) and the solution was heated in a closed vial at 100 °C overnight. The complex formation was evident from colour change (green to violet) and MS (*m/z* (ESI) +445.2 ([M+H]$^+$, $C_{12}H_{29}N_4NiO_6P_2^+$ requires 445.1), –443.0 ([M–H]$^-$, $C_{12}H_{27}N_4NiO_6P_2^-$ requires 443.1)). The solution was concentrated to ~0.5 ml. Violet plates of *trans*-O,O-[Ni(H_3L)]Cl·H_2O were formed by a slow vapour diffusion of acetone and analyzed by X-ray crystallography.

Preparation of {*trans*-O,O-[Ni(H_2L)]}$_3$·5H_2O

Ligand (50 mg of H_4te2p^{1,4}·4H_2O, 0.11 mmol) was dissolved in water (2 ml) and mixed with excess of freshly prepared Ni(OH)$_2$ (prepared from 52 mg of $NiCl_2$·6H_2O by addition of diluted aqueous NaOH and centrifugation). The solution was stirred overnight at room temperature and unreacted Ni(OH)$_2$ was filtered off. The complex formation was evident from colour of the solution (violet) and MS (*m/z* (ESI) +445.2 ([M+H]$^+$, $C_{12}H_{29}N_4NiO_6P_2^+$ requires 445.1), –443.0 ([M–H]$^-$, $C_{12}H_{27}N_4NiO_6P_2^-$ requires 443.1)). The single crystals – violet-blue plates – of {*trans*-O,O-[Ni(H_2L)]}$_3$·5H_2O were formed by a slow vapour diffusion of acetone.

Crystallography

Selected crystals were mounted on a glass fibre in random orientation and cooled to 150(1) K. The diffraction data were collected employing a Nonius Kappa CCD diffractometer (Enraf-Nonius) using Mo-*K*α (λ = 0.71073 Å) at 150(1) K (Cryostream Cooler Oxford Cryosystem) and analyzed using the HKL DENZO program package.[28] The structures were solved by direct methods and refined by full-matrix least-squares techniques (SIR92 (ref.[29]) and SHELXL97 (ref.[30])). The used scattering factors for neutral atoms were included in the SHELXL97 program.

In the structure of **1**·2HCl, all non-hydrogen atoms were refined anisotropically. The hydrogen atoms attached to carbon and nitrogen atoms were located in the electron density difference map; however, the hydrogen atoms attached to carbon atoms were fixed in theoretical positions using U_{eq}(H) = 1.2U_{eq}(C).

In the structure of **3**·4HBr·2H_2O, an independent unit is formed by one half of the amine molecule (the molecule lays on crystallographic double-fold axis), two bromide anions and one solvate water molecule. The bromide anions occupy three positions (one with full and two with crystallographic half occupancies). Most of hydrogen atoms were located in the electron density difference map; however, due to presence of a heavy atom, all hydrogen atoms were fixed in theoretical (C–H, N–H) or original (O–H) positions using U_{eq}(H) = 1.2U_{eq}(X). Due to a high absorption coefficient, absorption correction (Gaussian integration)[31] with scaling factors T_{min} = 0.2902 and T_{max} = 0.7003 was applied.

In the structure of *trans*-O,O-[Ni(H_3L)]Cl·H_2O, all non-hydrogen atoms were refined anisotropically. The hydrogen atoms were located in the electron density difference map; however, due to presence of a heavy atom, all hydrogen atoms were fixed in theoretical (C–H, N–H) or original (O–H) positions using U_{eq}(H) = 1.2U_{eq}(X).

In the structure of {*trans*-O,O-[Ni(H_2L)]}$_3$·5H_2O, three

complex molecules and five water solvate molecules form the structurally independent unit. All non-hydrogen atoms were refined anisotropically (except of those belonging to the disordered phosphonate) and the hydrogen atoms attached to carbon and nitrogen atoms were fixed in theoretical positions using $U_{eq}(H) = 1.2U_{eq}(X)$. One phosphonate pendant group was best refined as disordered in two positions (with the common carbon and nickel-coordinated oxygen atoms). A low-quality of crystal data and a high number of refined parameters led to high uncertainties; therefore, some atoms have relatively high thermal parameters and, so, the hydrogen atoms of water solvate molecules could not be located in the electron density map.

Crystal data

1·2HCl, $C_{12}H_{24}Cl_2N_4O_2$, M = 327.25, monoclinic, a = 9.6533(3), b = 15.5059(4), c = 10.3121(2) Å, β = 93.5297(16)°, U = 1540.62(7) Å^3, space group $P2_1/c$ (no. 14), Z = 4, 3533 reflections measured, 2869 unique, the final wR_2 = 0.0798 (all data). CCDC-XXXX.

3·4HBr·2H_2O, $C_{24}H_{44}Br_4N_4O_2$, M = 740.27, monoclinic, a = 7.27000(10), b = 20.5765(4), c = 20.0208(4) Å, β = 99.6839(13)°, U = 2952.26(9) Å^3, space group $C2/c$ (no. 15), Z = 4, 3408 reflections measured, 2854 unique, the final wR_2 = 0.0659 (all data). CCDC-XXXX.

trans-O,O-[Ni(H_3L)]Cl·H_2O, $C_{12}H_{31}ClN_4NiO_7P_2$, M = 499.51, orthorhombic, a = 7.9420(2), b = 9.4016(3), c = 27.8565(8) Å, U = 2079.98(10) Å^3, space group $P2_12_12_1$ (no. 19), Z = 4, 4739 reflections measured, 4236 unique, the final wR_2 = 0.0872 (all data). CCDC-XXXX.

{*trans*-O,O-[Ni(H_2L)]}$_3$·5H_2O, $C_{36}H_{94}N_{12}Ni_3O_{23}P_6$, M = 1425.18, hexagonal, a = 15.2662(1), c = 43.2280(4) Å, U = 8724.84(11) Å^3, space group $P6_1$ (no. 169), Z = 6, 13307 reflections measured, 9407 unique, the final wR_2 = 0.1673 (all data). CCDC-XXXX.

Potentiometric titrations

Equilibrium in systems of the ligand in free form (protonation study) and with Ca(II), Cu(II), Zn(II), Cd(II) and Pb(II) were established fast and, thus, they could be studied by conventional titrations. Titrations were carried out in a thermostatted vessel at 25.0±0.1 °C, at constant ionic strength $I(KNO_3)$ = 0.1 M, using a PHM 240 pH-meter, a 2 ml ABU 900 automatic piston burette and a GK 2401B combined electrode (all Radiometer). The concentration of the ligand was approximately 0.004 M. The ligand-to-metal ratio was 1:1 in all cases and the initial volume was about 5 ml. The measurements were taken with an addition of excess of HNO_3 to the mixture. The starting value of $-\log[H^+]$ was typically 1.65 (the Cu(II) system) or 1.8 (other systems). The mixtures were titrated with the solution of KOH till $-\log[H^+]$ of about 12.5. Titrations of each system were carried out at least four times. Each titration consisted of about 40 points (with approximately the same number of data points in both acid and alkaline regions). An inert atmosphere was ensured by a constant passage of argon saturated with water vapour.

The complexation reaction was too slow to be followed by standard titrations in the Ni(II) system. Thus, this system was studied by the "out-of-cell" method. Three titrations were done, each consists from 30 points (*i.e.* from 30 solutions mixed separately in test tubes). Initial volume of the samples was about 1 ml. The tubes were left firmly closed for 1 h, then an appropriate amount of the KOH solution was added and the tubes were tightly closed. The potential was then determined with freshly calibrated electrode after 3 weeks.

The water ion product was taken from literature (pK_w = 13.78).[32] The constants with their standard deviations were calculated with the OPIUM program package.[33] The program minimises the criterion of the generalised least-squares method using the calibration function

$$E = E_0 + S\times\log[H^+] + j_1\times[H^+] + j_2\times K_W/[H^+],$$

where the additive term E_0 contains the standard potentials of the electrodes used and the contributions of inert ions to the liquid-junction potential. Term S corresponds to the Nernstian slope and the $j_1\times[H^+]$ and $j_2\times[OH^-]$ terms are contributions of the H^+ and OH^- ions to the liquid-junction potential. They cause a deviation from a linear dependence between E and $-\log[H^+]$ only in strongly acidic or strongly alkaline solutions. The calibration parameters were determined from titration of the standard HNO_3 with the standard KOH solutions before and after every titration of ligand (ligand/metal ion system) to give calibration-titration pairs used for calculations of the constants. The protonation constants β_h are defined as concentration constants $\beta_h = [H_hL]/([H]^h\times[L])$. The concentration stability constants β_{hlm} are defined by the equation $\beta_{hlm} = [H_hL_lM_m]/([H]^h\times[L]^l\times[M]^m)$. In the definitions, the charges of the species are omitted for clarity.

NMR titrations

The ^{31}P NMR titration experiments for determination of the highest protonation constants of the ligand ($-\log[H^+]$ 11.6–13.5) were carried out by recommended method[34] under the conditions of potentiometric titrations (H_2O, 0.1 M KNO_3, 25.0 °C, 0.004 M ligand); however, with no control of ionic strength at the last points above $-\log[H^+]$ 13. A coaxial capillary with D_2O was used for a lock. Protonation constant was calculated with OPIUM from the dependence of δ_P on $-\log[H^+]$.

Results and Discussion

Syntheses

Originally, H_4te2p[1,4] was prepared *via* thiophosphonyl-bis(amide) protection of 1,4-positions of the cyclam ring,[25] but scaling up the synthesis was complicated due to extensive chromatographic purifications. Thus, we proposed a new synthetic pathway, employing known oxalyl-bis(amide)- and bis(benzyl)-protected cyclams **1**, **2** and **3**.[26] However, in the original article, the authors isolated the oxalylcyclam **1** by simple crystallization which did not work in our hands. Therefore, we decided to isolate the compound **1** in the form of dihydrochloride which precipitated easily from ethanol solution of **1** on addition of conc. aq. HCl. The dibenzylcyclam **3** was isolated after crystallization from conc. aq. HBr acid as **3**·4HBr·4H_2O. Originally, we tried the crystallization from conc. aq. HCl, but the hydrochloride precipitated in an extremely fine form and, thus, was hardly

filterable. The dibenzylcyclam **3** reacted with triethyl phosphite and paraformaldehyde forming protected intermediate **4** in a quantitative yield (according to ^{31}P NMR). After removal of excess formaldehyde and phosphite, the protecting benzyl groups as well as phosphonate ethyl ester groups were cleaved. First, we tried reductive debenzylation of the ester **4** in presence of Pd/C. This procedure led to a complicated mixture of products instead of pure compound **6**. Further hydrolysis of ester moieties (HBr/AcOH) resulted in inseparable mixture of products. Therefore, the ester groups were hydrolyzed first to obtain acid **5** and benzyl groups were removed in the last step to obtain H_4te2p[1,4] in an overall moderate yield.

Crystal structures

Crystal structure of 1·2HCl

Compound 1·2HCl crystallized in the form of colourless needles. Independent unit of the crystal structure is formed by one macrocyclic molecule and two chloride counter-ions. Six-membered cycle (Fig. 1) formed by oxalyl group bounded to macrocycle nitrogen atoms N1 and N4 is perpendicular to the plane of the rest of the macrocycle. The crystal structure is stabilized by intermolecular hydrogen bond network between protonated amino groups, chloride anions ($d_{N\cdots Cl}$ ~3.0–3.1 Å) and oxygen atoms belonging to the neighbouring molecule ($d_{N\cdots O\#}$ ~2.8–2.9 Å).

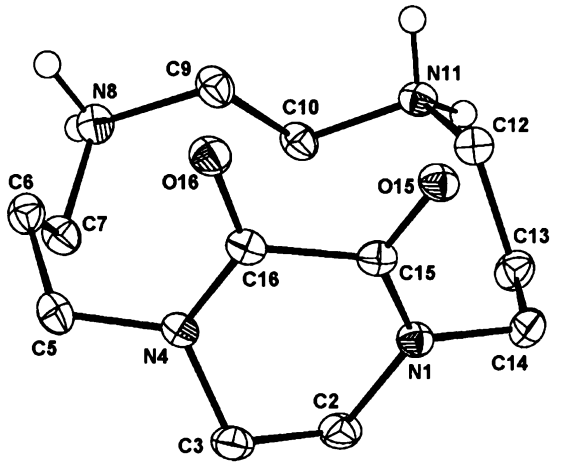

Fig. 1 Molecular structure of the $H_2$1^{2+} dication found in the crystal structure of 1·2HCl. Hydrogen atoms on carbon atoms are omitted for the sake of clarity. Thermal ellipsoids show 50 % probability level.

Crystal structure of 3·4HBr·2H$_2$O

In the structure of 3·4HBr·2H_2O, all amino groups are protonated. The macrocycle is in the most common rectangular conformation (3,4,3,4)-A with all amino groups laying in the corners of the rectangle (Fig. 2).[2] Whole structure is stabilized by intermolecular hydrogen bonds between protonated amino groups, bromide anions ($d_{N\cdots Br}$ ~3.2 Å) and oxygen atom of solvate water molecule ($d_{N\cdots O}$ ~2.7 Å). There are also contacts between solvate water hydrogen atoms and the bromides ($d_{O\cdots Br}$ ~3.3–3.4 Å).

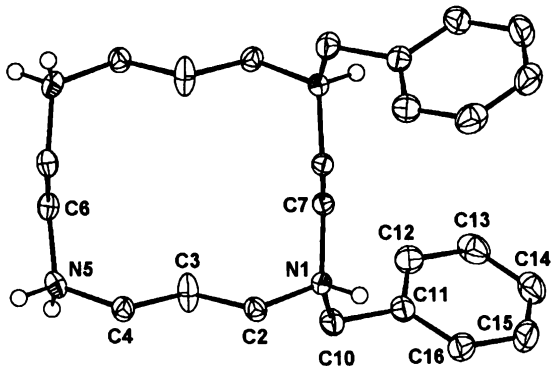

Fig. 2 Molecular structure of the $H_4$3^{4+} tetracation found in the crystal structure of 3·4HBr·2H_2O. Hydrogen atoms on carbon atoms are omitted for the sake of clarity. Thermal ellipsoids show 50 % probability level.

Crystal structure of *trans*-O,O-[Ni(H_3L)]Cl·H_2O

The independent unit is formed by a complex molecule, a chloride anion and a solvate water molecule. Coordination sphere of Ni(II) ion is octahedral, with four macrocycle nitrogen atoms in the equatorial plane and two apically coordinated oxygen atoms of the phosphonate pendant arms (Fig. 3). Coordination bond lengths have common values for these types, with slightly longer bonds (by ~0.06 Å) between central ion and the tertiary amino groups comparing to the secondary ones (Table 1). The macrocycle is in the most stable configuration **III**,[35] which is the most common configuration found for Ni(II) complexes with cyclam-like ligands.[36] The geometries around phosphorus atoms are roughly tetrahedral. One phosphonate is monoprotonated, and the other is double-protonated on the non-coordinated oxygen atoms. The isolation of such species points to a high inertness of the complex, as the second protonation step of the coordinated phosphonate group proceeds typically with pK_a ~1.[23,37,38] Similar over-protonated species were isolated also in the case of Ni(II) complexes of H_4te2p[1,8].[37] The orientation of phosphonate pendant arms above and below the macrocyclic plane is fixed by intramolecular hydrogen bonds between hydrogen atom of secondary amino group (hydrogen atoms attached to N8 and N11) and uncoordinated oxygen atom of the phosphonates (O23 and O12, respectively) with intermediate lengths ($d_{N\cdots O}$ ~2.9 Å). The complex molecules are connected to infinite chains *via* a very short intermolecular hydrogen bond between one –OH group of double-protonated phosphonate (O12) and non-protonated oxygen atom of the second phosphonate pendant of neighbouring molecule (O23$^{\#}$) with O12···O23$^{\#}$ separation of 2.41 Å. Similar short hydrogen bonds connecting the neighbouring units were observed also in the structures of *trans*-O,O-[Co(Hte2p[1,8])]·6H_2O (ref.[38]) and *trans*-O,O-[Cu(H_2te2p[1,8])]·2H_2O (ref.[23]) complexes. Further hydrogen bond network is formed between protonated phosphonates, the water solvate and the chloride anion.

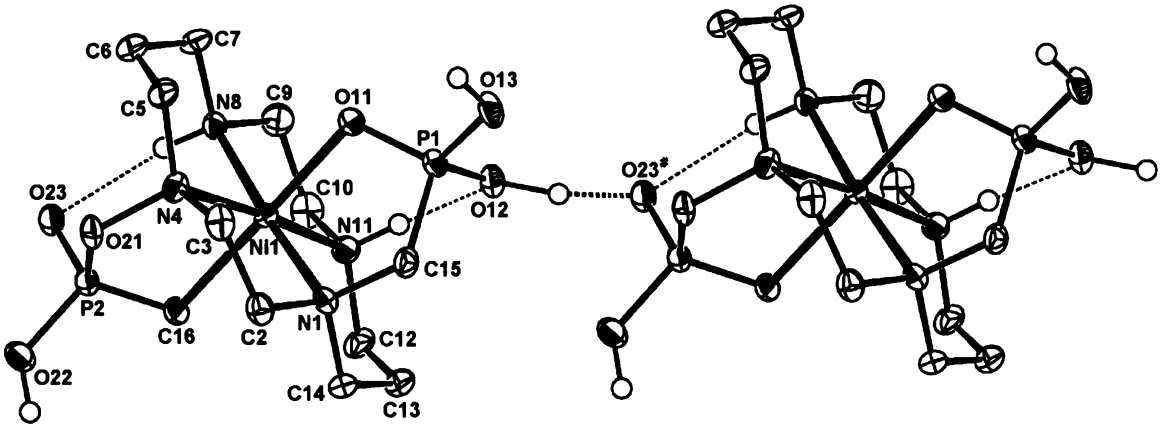

Fig. 3 Molecular structure of the complex units found in the crystal structure of *trans*-O,O-[Ni(H_3L)]Cl·H_2O, showing hydrogen bond system (dashed). Hydrogen atoms attached to carbon atoms are omitted for the sake of clarity. Thermal ellipsoids show 50 % probability level.

Table 1 Selected geometric parameters of the nickel(II) coordination spheres in the crystal structures of *trans*-O,O-[Ni(H_3L)]Cl·H_2O and {*trans*-O,O-[Ni(H_2L)]}$_3$·5H_2O.

	trans-O,O-[Ni(H_3L)]Cl·H_2O	{*trans*-O,O-[Ni(H_2L)]}$_3$·5H_2O		
		distances (Å)		
		molecule A	molecule B	molecule C
Ni1–N1	2.130(3)	2.14(1)	2.13(1)	2.16(1)
Ni1–N4	2.136(3)	2.09(1)	2.10(1)	2.13(1)
Ni1–N8	2.076(3)	2.06(1)	2.06(1)	2.07(1)
Ni1–N11	2.076(3)	2.08(1)	2.07(1)	2.08(1)
Ni1–O11	2.106(2)	2.14(1)	2.14(1)	2.09(1)
Ni1–O21	2.119(2)	2.09(1)	2.09(1)	2.10(1)
		angles (°)		
N1–Ni1–N4	86.5(1)	86.6(4)	88.5(3)	86.1(5)
N1–Ni1–N8	175.4(1)	176.7(5)	173.1(5)	174.7(4)
N1–Ni1–N11	94.1(1)	95.7(4)	93.8(5)	94.6(5)
N1–Ni1–O11	86.1(1)	86.7(5)	85.3(5)	94.6(5)
N1–Ni1–O21	91.8(1)	91.3(5)	93.1(5)	93.1(4)
N4–Ni1–N8	94.5(1)	91.9(5)	91.6(5)	93.3(5)
N4–Ni1–N11	175.5(1)	172.9(6)	174.9(5)	176.8(5)
N4–Ni1–O11	94.1(1)	95.1(6)	93.3(5)	90.1(4)
N4–Ni1–O21	85.7(1)	84.7(6)	86.2(5)	86.3(4)
N8–Ni1–N11	85.3(1)	86.1(3)	86.8(3)	86.3(5)
N8–Ni1–O11	89.3(1)	90.5(5)	87.9(4)	86.3(5)
N8–Ni1–O21	92.7(1)	91.4(4)	93.8(3)	92.2(4)
N11–Ni1–O11	93.3(1)	91.7(4)	91.5(4)	93.2(4)
N11–Ni1–O21	89.9(1)	88.5(5)	89.0(5)	90.5(5)
O11–Ni1–O21	176.3(1)	178.1(5)	178.3(4)	176.3(4)

Crystal structure of {*trans*-O,O-[Ni(H_2L)]}$_3$·5H_2O

The independent unit is formed by three complex molecules and five solvate water molecules. Coordination spheres of all nickel(II) ions are very similar to each other and to the previous complex, with four macrocycle nitrogen atoms in equatorial (with configuration **III**) and two phosphonate oxygen atoms in axial positions. Coordination bond lengths have common values for these types, with slightly longer bonds (by ~0.06 Å) between central ion and the tertiary amino groups comparing to the secondary ones (Table 1). In a summary, a low quality of the diffraction data led to high uncertainties of atom positions and high anisotropic displacement parameters. However, the complex stereochemistry was unambiguously determined.

Ligand protonation

The first two dissociation constant of the azacycle amino groups having phosphonic acid pendants arms are usually very high (pK_a ~13),[39] *i.e.* the values lay out of the region of potentiometric titrations and, thus, they cannot be determined by this method. Therefore, ^{31}P NMR titration was employed to obtain the values of logβ_{11} and logβ_{21}. However, only the value of logβ_{21} constant could be fitted. This fact can be attributed to lower precision of data due to non-constant ionic strength at –log[H^+] >12.5 and/or a relatively low number of data points (comparing to potentiometry). In addition, such behaviour can point to a "reverse order" of protonation (dissociation) constants.[22] The presence of strong hydrogen bonds in the system is evidenced from appearance of ^{1}H NMR spectra at different solution pH. The signals are broad in pH region 3–13 (where the macrocyclic amine groups bind just

two protons). The corresponding overall protonation constant $\log\beta_{21}$ is higher than that observed for cyclam and acetate analogues, as it is typical for aminomethylphosphonic acids.[39,42,43] The third and fourth protons are attached to an oxygen atom of phosphonate moieties, with the values of the dissociation constants (pK_a's 6.56 and 5.19) typical for such dissociation.[39,42,43]

The final values of protonation (dissociation) constants were obtained from simultaneous fitting of both ^{31}P NMR and potentiometry data and are compiled in Table 2.

Table 2 Protonation[a] constants of $H_4te2p^{1,4}$ and dissociation[b] constants of $H_4te2p^{1,4}$ and related ligands (Chart 1; 25.0 °C, $I(KNO_3)$ = 0.1 M).

	$\log\beta_h$ [a]					pK_a [b]			
h	$H_4te2p^{1,4}$	Equilibrium[c]	$H_4te2p^{1,4}$	Cyclam [41]	H_2te1p [21]	H_1te1a [14a]	$H_4te2p^{1,8}$ [22]	H_8tetp [40]	H_4teta [44]
1	–	$HL \leftrightarrow H^+ + L$	–	11.29	12.49	12.18	–	–	10.58
2	*25.72(3)*[d]	$H_2L \leftrightarrow H^+ + HL$	*25.72* [d]	10.19	11.76	10.87	*26.41* [d]	*25.28* [d]	10.17
3	32.28(1)	$H_3L \leftrightarrow H^+ + H_2L$	6.56	1.61	6.05	3.01	6.78	8.85	4.09
4	37.47(1)	$H_4L \leftrightarrow H^+ + H_3L$	5.19	1.91	2.42	<2	5.36	7.68	3.35
5	39.77(1)	$H_5L \leftrightarrow H^+ + H_4L$	2.30	–	–	<2	1.15	6.23	–
6	–	$H_6L \leftrightarrow H^+ + H_5L$	–	–	*2.16* [d]	–	–	5.33	–

[a] $\beta_h = [H_hL]/([H]^h \times [L])$. [b] $K_a = ([H] \times [H_{n-1}L])/[H_nL]$. [c] Charges of species are omitted for clarity reason. [d] Values *in italics* correspond to the protonation/dissociation over two steps.

Stability of complex species

In all studied systems, the ligand forms 1:1 complex species which can be additionally mono- and double-protonated. In the systems with Pb(II), triple-protonated species was also detected in a low abundance at $-\log[H^+]$ 4–7. The results are compiled in Table 3.

In the case of calcium(II), the value of $\log\beta_{011}$ is low, pointing to a very low abundance of the complex species in solution. The initially formed diprotonated complex $[Ca(H_2L)]$ probably loses protons from nitrogen atoms of the macrocycle, as can be seen from the pK_a's of 12.12 and 11.92. Thus, the metal ion is probably coordinated only by the oxygen atoms of the phosphonate pendant moiety in double-protonated complex, and macrocyclic part starts to coordinate only after the full deprotonation in very alkaline solutions. Similar coordination behaviour was found also for $H_4te2p^{1,8}$ (ref.[45]) and H_2te1p (ref.[21]).

In the case of lead(II) complexation, the value of $\log\beta_{011}$ is much higher than that found for Ca(II), and the abundances of complex species are also higher. Free lead(II) ion is not present in the equimolar mixture above pH ~8. The complexation starts with formation of triprotonated complex $[Pb(H_3L)]^+$, which have maximal abundance at pH ~5. According to its pK_a (5.29), it loses proton probably from the phosphonate pendant arm. The second pK_a (6.39) is also comparable to the values corresponding to phosphonate moieties, but the last one is much higher (10.20). It suggests two possible explanations. In the first case, two oxygen atoms (one of each pendant arm) are protonated as well as one nitrogen atom of the macrocycle in the triple-protonated complexes. In such case, at least other nitrogen atoms of the macrocycle should be involved in metal coordination in the $[Pb(H_2L)]$ species; but such species exists even at pH below 5, and such coordination of the macrocycle nitrogen atom would be very unusual. The second possibility suggests that the metal ion is bound only by pendant arms in the triple-protonated complex and two macrocycle nitrogen atoms are still protonated. In this case, due to a higher affinity of Pb(II) for nitrogen coordination (comparing to the Ca(II) complex), the pK_a value corresponding to $[Pb(H_2L)]$ species would be lowered by several orders of magnitude compared to those of the free ligand. Furthermore, as the X-ray diffraction study of the solid phase formed from Pb(II)–$H_4te2p^{1,8}$ system at pH ~6 revealed Pb(II) coordination by only phosphonate groups and protonation of two nitrogen atoms.[45] So, the second alternative of proton locations seems to be correct.

In the systems with transition metal ions (Ni(II), Cu(II), Zn(II) and Cd(II)), the high values of the $\log\beta_{011}$ and the values of the pK_a clearly show that all four nitrogen atoms are coordinated in all complex species, and the coordination sphere is probably closed by at least one of phosphonate pendant arm. The protonation of these complexes takes place on the non-coordinated phosphonate oxygen atoms (see also above for the crystal structure of Ni(II) complex). The first protonation occurs with pK_a's slightly higher (6.81 for Cu(II), 6.88 for Zn(II) and 7.80 for Cd(II)) or slightly lower (6.14 for Ni(II)) than the corresponding pK_a value of the free ligand (6.56). The second protonations occur with lower pK_a's comparing to that of the free ligand. The similar drop of pK_a values of phosphonate pendant arm upon coordination was observed also for analogous complexes of $H_4te2p^{1,8}$ (refs[23,45]) and H_2te1p (ref.[21]).

The highest stability was found for the Cu(II) complex, as it commonly reflects the Irving-Williams trend and, in addition, the optimal size of the cyclam ring for this cation. The complexation of Cu(II) starts in acidic region and the metal ion is fully encapsulated in the complex below pH ~3 (Fig. 4). The selectivity of the ligand for Cu(II) is very high as the difference between corresponding stability constants is about seven and five orders of magnitude for Cu/Zn and Cu/Ni pairs, respectively. These facts are very promising for a potential analytical or radiopharmaceutical use.

Table 3 Stability constants of complexes of $H_4te2p^{1,4}$ with selected metal ions (25.0 °C, $I(KNO_3)$ = 0.1 M).

Cation	h	l	m	$\log\beta_{hlm}$ [a]	pK_a [b]
Ni(II)	0	1	1	21.92(6)	–
	1	1	1	28.06(6)	6.14
	2	1	1	33.18(3)	5.12
Cu(II)	0	1	1	27.21(3)	–
	1	1	1	34.02(3)	6.81
	2	1	1	38.93(2)	4.91
Zn(II)	0	1	1	20.16(3)	–
	1	1	1	27.04(1)	6.88
	2	1	1	31.47(4)	4.43
Cd(II)	0	1	1	17.03(2)	–
	1	1	1	24.83(1)	7.80
	2	1	1	29.75(3)	4.92
Pb(II)	0	1	1	12.85(4)	–
	1	1	1	23.05(3)	10.20
	2	1	1	29.44(3)	6.39
	3	1	1	34.73(9)	5.29
Ca(II)	0	1	1	3.42(5)	–
	1	1	1	15.34(9)	11.92
	2	1	1	27.46(5)	12.12

[a] $\beta_{hlm} = [H_hL_lM_m]/([H]^h\times[L]^l\times[M]^m)$, [b] $K_a = ([H]\times[M(H_{h-1}L)])/[M(H_hL)]$.

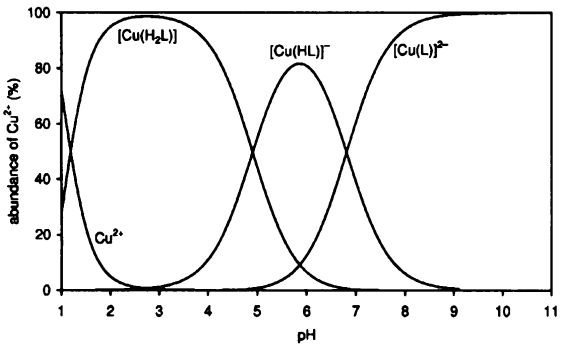

Fig. 4 Distribution diagram for the Cu(II)-$H_4te2p^{1,4}$ system ($c_L = c_{Cu}$ = 0.004 M).

From the comparison of stability constants determined for the title ligand and the related compounds (Table 4), it is clear, that the cyclam skeleton substituted by several (few) pendant arms based on phosphorus acid is a good choice as the ligands have a high selectivity of copper(II) complexation. In the $H_4te2p^{1,4}$ case, the complexation of copper(II) is more selective comparing to its 1,8-isomer[23] and the monophosphonate derivative H_2te1p.[21] Furthermore, the complexation reaction is relatively fast (similarly to the 1,8-isomer) in slightly acid solutions, and much faster than that of the monophosphonate ligand, H_2te1p,[21] and cyclam[46] itself; it points to an acceleration effect of more phosphonate pendant arms. The concentration of free Cu(II) ion in the Cu(II)-$H_4te2p^{1,4}$ system (expressed as pCu = –log[Cu(II)] calculated for an equimolar ligand-Cu(II) mixture) is about one order of magnitude lower than that for the 1,8-isomer and more close to values for other ligands with coordinating pendant arms (Table 4). However the lower pCu values for the phosphorus-containing ligands are mainly given by the very high overall basicity of the ligands. The kinetics of complex formation and dissociation is under study.

Table 4 Comparison of stability constants ($\log\beta_{011}$) of the [M(L)] complex species formed with $H_4te2p^{1,4}$ and related ligands.

ligand\ion	Ni(II)	Zn(II)	Cd(II)	Pb(II)	Ca(II)	Cu(II)	pCu [a]
$H_4te2p^{1,4}$	21.92	20.16	17.03	12.85	3.45	27.21	9.4
$H_4te2p^{1,8}$ [b]	21.99	20.35	17.89	14.96	5.26	25.40	8.1
H_2te1p [c]	–	21.03	15.91	–	3.07	27.34	10.1
cyclam [d]	22.2	15.2	11.3	10.9	–	28.1	11.9
H_4teta [e]	19.91	16.62	18.25	14.3	8.42	21.74	9.1
H_8tetp	–	17.6[f]	16.7[f]	15.5[f]	–	25.99[g]	8.4

[a] Calculated for –log[H+] = 7.4 and $c_L = c_M$ = 0.004 M. [b] ref.[23,45]. [c] ref.[21]. [d] ref.[47]. [e] ref.[47] [f] ref.[48] [g] ref.[44b]

Conclusions

The title ligand, $H_4te2p^{1,4}$, forms extremely stable complex with Cu(II) ($\log\beta$(CuL) = 27.21) with a high selectivity of complexation over other metal ions (*i.e.* $\log\beta$(ZnL) = 20.16, $\log\beta$(NiL) = 21.92). The complexation of copper(II) proceeds relatively fast as it could be determined by conventional potentiometric titration. It makes the ligand promising as the parent chelator for possible radiopharmaceutical applications. The ligand forms octahedral *trans*-O,O Ni(II) complexes with the most stable macrocycle configuration **III**. From acid solution, the crystals of *trans*-O,O-$[Ni(H_3L)]Cl\cdot H_2O$ were isolated with mono- and double-protonated phosphonate pendant arms. The isolation of such species points to a high inertness of the complex. From neutral solutions, the crystals of $\{trans\text{-O,O-}[Ni(H_2L)]\}_3\cdot 5H_2O$ were isolated where each pendant arm is monoprotonated.

Acknowledgement

This work was supported by the Grant Agency of the Czech Republic (203/06/0467), the Ministry of Education and Youth of Czech Republic (MSM0021620857) and COST D38.

Notes and references

[a] *Department of Inorganic Chemistry, Universita Karlova (Charles University), Hlavova 2030, Prague 2, 128 40, Czech Republic. Tel: +420-2-2195-1261; Fax: +420-2-2195-1253; E-mail: modrej@natur.cuni.cz*

† Electronic Supplementary Information (ESI) available: scheme of the ligand synthesis; molecular structures of the $[Ni(H_2L)]$ complex units; NMR spectra of H_4L at different pH; distribution diagrams of the free ligand and the M(II)-$H_4te2p^{1,4}$ systems (M = Ca, Pb, Ni, Zn, Cd). See DOI: 10.1039/b000000x/

1 (*a*) A. E. Martell and R. D. Hancock, *Metal Complexes in Aqueous Solutions*, Plenum Press, New York, 1996; (*b*) K. P. Wainwright, *Coord. Chem. Rev.*, 1997, 166, 35–90; (*c*) S. F. Lincoln, *Coord. Chem. Rev.*, 1997, **166**, 255–289; (*d*) L. F. Lindoy, *Adv. Inorg. Chem.*, 1998, **45**, 75–125. (*e*) R Delgado, V. Félix, L. M. P. Lima and D. W. Price, *Dalton Trans.*, **2007**, 2734–2745.

2 M. Meyer, V. Dahaoui-Ginderey, C. Lecomte and R. Guilard, *Coord. Chem. Rev.*, 1998, **178-180**, 1313–1405.

3 X. Liang and P. J. Sadler, *Chem. Soc. Rev.*, 2004, **33**, 246–266.

4 E. De Clercq, *Nat. Rev. Drug Discov.*, 2003, **2**, 581–587.

5 (*a*) G. J. Bridger and R. T. Skerlj, *Adv. Antiviral Drug Des.*, 1999, **3**, 161–229; (*b*) X. Liang, J. A. Parkinson, M. Weishaupl, R. O. Gould, S. J. Paisey, H. S. Park, T. M. Hunter, C. A. Blindauer, S. Parsons and P. J. Sadler, *J. Am. Chem. Soc.*, 2002, **124**, 9105–9112; (*c*) L. O. Gerlach, J. S. Jakobsen, K. P. Jensen, M. R. Rosenkilde, R. T. Skerlj,

U. Ryde, G. J. Bridger and T. W. Schwartz, *Biochemistry*, 2003, **42**, 710–717.

6 (*a*) S. Liu and D. S. Edwards, *Bioconjugate Chem.*, 2001, **12**, 7–34; (*b*) S. Liu and D. S. Edwards, *Top. Curr. Chem.*, 2002, **222**, 259–278; (*c*) *Handbook of Radiopharmaceuticals. Radiochemistry and Applications*, ed. M. J. Welch and C. S. Redvanly, Wiley, 2003; (*d*) S. Liu, *Chem. Soc. Rev.*, 2004, **33**, 445–461; (*e*) W. P. Li, L. A. Meyer and C. J. Anderson, *Top. Curr. Chem.*, 2005, **252**, 179–192.

7 (*a*) R. B. Wilder, G. L. DeNardo and S. J. DeNardo, *J. Clin. Oncol.*, 1996, **14**, 1383–1400; (*b*) I. Novak-Hofer and P. A. Schubiger, *Eur. J. Nucl. Med.*, 2002, **29**, 821–830; (*c*) S. V. Smith, *J. Inorg. Biochem.*, 2004, **98**, 1874–1901; (*d*) X. Sun and C. J. Anderson, *Methods Enzymol.*, 2004, **386**, 237–261; (*e*) T. J. Wadas, E. H. Wong, G. R. Weisman and C. J. Anderson, *Curr. Pharm. Des.*, 2007, **13**, 3–16.

8 M. K. Moi, C. F. Meares, M. J. McCall, W. C. Cole and S. J. DeNardo, *Anal. Biochem.*, 1985, **148**, 249–253.

9 (*a*) A. Riesen, M. Zehnder and T. A. Kaden, *Acta Crystallogr.*, 1988, **C44**, 1740-1742; (*b*) E. Espinosa, M. Meyer, D. Berard, R. Guilard, *Acta Crystallogr.*, 2002, **C58**, m119–m121; (*c*) J. D. Silversides, C. C. Allan and S. J. Archibald, *Dalton Trans.*, **2007**, 971–978.

10 L. A. Bass, M. Wang, M. J. Welch and C. J. Anderson, *Bioconjugate Chem.*, 2000, **11**, 527–532.

11 (*a*) F. I. Belskii, Y. M. Polikarpov and M. I. Kabachnik, *Usp. Khim.*, 1992, **61**, 415–455; (*b*) C. F. G. C. Geraldes, M. P. M. Marques, B. de Castro and E. Pereira, *Eur. J. Inorg. Chem.*, **2000**, 559–565; (*c*) X. Sun, M. Wuest, Z. Kovacs, A. D. Sherry, R. Motekaitis, Z. Wang, A. E. Martell, M. J. Welch and C. J. Anderson, *J. Biol. Inorg. Chem.* 2003, **8**, 217–225.

12 (*a*) I. Lázár, A. D. Sherry, R. Ramasamy, E. Brücher and R. Kiraly, *Inorg. Chem.*, 1991, **30**, 5016–5019; (*b*) K. Bazakas and I. Lukeš, *J. Chem. Soc., Dalton Trans.*, **1995**, 1133–1137; (*c*) J. Rohovec, M. Kývala, P. Vojtíšek, P. Hermann and I. Lukeš, *Eur. J. Inorg. Chem.*, **2000**, 195–203; (*d*) P. Lubal, M. Kývala, P. Hermann, J. Holubová, J. Rohovec, J. Havel and I. Lukeš, *Polyhedron*, 2001, **20**, 47–55.

13 (*a*) E. K. Barefield and F. Wagner, *Inorg. Chem.*, 1973, **12**, 2435–2439; (*b*) L. Hertli and T. A. Kaden, *Helv. Chim. Acta*, 1974, **57**, 1328–1333.

14 (*a*) M. Studer and T. A. Kaden, *Helv. Chim. Acta*, 1986, **69**, 2081–2086; (*b*) D. Tschudin, A. Basal and T. A. Kaden, *Helv. Chim. Acta*, 1988, **71**, 100–106.

15 D. Tschudin, A. Riesen and T. A. Kaden, *Helv. Chim. Acta*, 1989, **72**, 313–319.

16 (*a*) I. M. Helps, D. Parker, J. Chapman and G. Ferguson, *J. Chem. Soc., Chem. Commun.*, **1988**, 1094–1095; (*b*) J. Chapman, G. Ferguson, J. F. Gallagher, M. C. Jennings and D. Parker, *J. Chem. Soc., Dalton Trans.*, **1992**, 345–353.

17 (*a*) A. Comparone and T. A. Kaden, *Helv. Chim. Acta*, 1998, **81**, 1765–1772; (*b*) L. Siegfried, A. Comparone, M. Neuburger and T. A. Kaden, *Dalton Trans.*, **2005**, 30–36.

18 C. Bucher, E. Duval, J.-M. Barbe, J.-N. Verpeaux, C. Amatore and R. Guilard, *C. R. Acad. Sci., Ser. IIc, Chem.*, 2000, **3**, 211–222.

19 (*a*) A. E. Goeta, J. A. K. Howard, D. Maffeo, H. Puschmann, J. A. G. Williams and D. S. Yufit, *J. Chem. Soc., Dalton Trans.*, **2000**, 1873–1880; (*b*) A. S. Batsanov, A. E. Goeta, J. A. K. Howard, D. Maffeo, H. Puschmann and J. A. G. Williams, *Polyhedron*, 2001, **20**, 981–986.

20 H. Kurosaki, C. Bucher, E. Espinosa, J.-M. Barbe and R. Guilard, *Inorg. Chim. Acta*, 2001, **322**, 145–149.

21 S. Fűzerová, J. Kotek, I. Císařová, P. Hermann, K. Binnemans and I. Lukeš, *Dalton Trans.*, **2005**, 2908–2915.

22 J. Kotek, P. Vojtíšek, I. Císařová, P. Hermann, P. Jurečka, J. Rohovec and I. Lukeš, *Collect. Czech. Chem. Commun.*, 2000, **65**, 1289–1316.

23 J. Kotek, P. Lubal, P. Hermann, I. Císařová, I. Lukeš, T. Godula, I. Svobodová, P. Táborský and J. Havel, *Chem. Eur. J.*, 2003, **9**, 233–248.

24 (*a*) I. Svobodová, P. Lubal, P. Hermann, J. Kotek and J. Havel, *Microchim. Acta*, 2004, **148**, 21–26; (*b*) I. Svobodová, P. Lubal, P. Hermann, J. Kotek and J. Havel, *J. Inclusion Phenom. Macrocyclic Chem.*, 2004, **49**, 11–15.

25 T. Vitha, J. Kotek, J. Rudovský, V. Kubíček, I. Císařová, P. Hermann and I. Lukeš, *Collect. Czech. Chem. Commun.*, 2006, **71**, 337–367.

26 F. Bellouard, F. Chuburu, N. Kervarec, L. Toupet, S. Triki, Y. Le Mest and H. Handel, *J. Chem. Soc., Perkin Trans. 1*, **1999**, 3499–3505.

27 (*a*) E. K. Barefield, *Inorg. Chem.*, 1972, **11**, 2273–2274; (*b*) I. Meunier, A. K. Mishra, B. Hanquet, P. Cocolios and R. Guilard, *Can. J. Chem.*, 1995, **73**, 685–695.

28 (*a*) Z. Otwinovski and W. Minor, *HKL Denzo and Scalepack Program Package* by Nonius BV, Delft, **1997**; (*b*) Z. Otwinovski and W. Minor, *Methods Enzymol.*, 1997, **276**, 307–326.

29 A. Altomare, M. C. Burla, M. Camalli, G. Cascarano, C. Giacovazzo, A. Guagliardi and G. Polidori, *J. Appl. Crystallogr.*, 1994, **27**, 435.

30 G. M. Sheldrick, *SHELXL97. Program for Crystal Structure Refinement from Diffraction Data*, University of Gottingen. Gottingen **1997**.

31 P. Coppens, in: *Crystallographic Computing*, ed. F. R. Ahmed, S. R. Hall and C. P. Huber, Copenhagen, Munksgaard, 1970, pp. 255–270.

32 C. F. Baes, Jr. and R. E. Mesmer, *The Hydrolysis of Cations*, Wiley, New York, 1976.

33 M. Kývala and I. Lukeš, *Chemometrics '95*, Abstract book p. 63. Pardubice, Czech Republic, **1995**; full version of *OPIUM program package* is available (free of charge) on http://www.natur.cuni.cz/~kyvala/opium.html.

34 K. Popov, H. Ronkkomaki and L. H. J. Lajunen, *Pure Appl. Chem.*, 2006, **78**, 663–675.

35 B. Bosnich, C. K. Poon and M. L. Tobe, *Inorg. Chem.*, 1965, **4**, 1102–1108.

36 (*a*) M. A. Donnelly and M. Zimmer, *Inorg. Chem.*, 1999, **38**, 1650–1658. (*b*) T. M. Hunter, S. J. Paisey, H.-S. Park, L. Cleghorn, A. Parkin, S. Parsons and P. J. Sadler, *J. Inorg. Biochem.*, 2004, **98**, 713–719.

37 J. Kotek, P. Vojtíšek, I. Císařová, P. Hermann and I. Lukeš, *Collect. Czech. Chem. Commun.*, 2001, **66**, 363–381.

38 J. Kotek, P. Hermann, I. Císařová, J. Rohovec and I. Lukeš, *Inorg. Chim. Acta*, 2001, **317**, 324–330.

39 I. Lukeš, J. Kotek, P. Vojtíšek and P. Hermann, *Coord. Chem. Rev.*, 2001, **216–217**, 287–312.

40 R. D. Hancock, R. J. Motekaitis, J. Mashishi, I. Cukrowski, J. H. Reibenspies and A. E. Martell, *J. Chem. Soc., Perkin Trans. 2*, **1996**, 1925–1929.

41 (*a*) R. Delgado, L. C. Siegfried and T. A. Kaden, *Helv. Chim. Acta*, 1990, **73**, 140–148; (*b*) F. Marques, L. Gano, M. P. Campello, S. Lacerda, I. Santos, L. M. P. Lima, J. Costa, P. Antunes and R. Delgado, *J. Inorg. Biochem.*, 2006, **100**, 270–280.

42 T. Kiss and I. Lázár, in: *Aminophosphonic and Aminophosphinic Acids. Chemistry and Biological Activity*, ed. V. P. Kukhar and H. R. Hudson, Wiley, 2000; ch. IX, pp. 285–326.

43 K. Popov, H. Rönkkömäki and L. H. J. Lajunen, *Pure Appl. Chem.*, 2001, **73**, 1641–1677.

44 (*a*) S. Chaves, R. Delgado and J. J. R. Frausto Da Silva, *Talanta*, 1992, **39**, 249–254; (*b*) R. Delgado, J. Costa, K. P. Guerra and L. M. P. Lima, *Pure Appl. Chem.*, 2005, **77**, 569–579.

45 I. Svobodová, P. Lubal, J. Plutnar, J. Havlíčková, J. Kotek, P. Hermann and I. Lukeš, *Dalton Trans.*, **2006**, 5184–5197.

46 R. J. Motekaitis, B. E. Rogers, D. E. Reichert, A. E. Martell and M. J. Welch, *Inorg. Chem.*, 1996, **35**, 3821–3827.

47 (*a*) A. E. Martell and R. M. Smith, *Critical Stability Constants*. Plenum Press, New York, 1974–1989, Vols. 1–6; (*b*) *NIST Standard Reference Database 46 (Critically Selected Stability Constants of Metal Complexes)*, Version 7.0, 2003.

48 S. A. Pisareva, F. I. Belskii, T. Ya. Medved and M. I. Kabachnik, *Izv. Akad. Nauk SSSR, Ser. Khim.*, **1987**, 413–417.